

Article

Performance Comparison of Advanced Transcritical Power Cycles with High-Temperature Working Fluids for the Engine Waste Heat Recovery

Xinxing Lin ¹, Chonghui Chen ², Aofang Yu ², Likun Yin ¹ and Wen Su ^{2,*} 

¹ Institute of Science and Technology, China Three Gorges Corporation, Beijing 100038, China; lin_xinxing@ctg.com.cn (X.L.); yin_likun@ctg.com.cn (L.Y.)

² School of Energy Science and Engineering, Central South University, Changsha 410083, China; chchen@csu.edu.cn (C.C.); yuaf923@csu.edu.cn (A.Y.)

* Correspondence: suwenzn@csu.edu.cn; Tel.: +86-0731-88879863

Abstract: To efficiently recover the waste heat of mobile engine, two advanced transcritical power cycles, namely split cycle and dual pressure cycle, are employed, based on the recuperative cycle. Performances of the two cycles are analyzed and compared through the development of thermodynamic models. Under given gas conditions, seven high-temperature working fluids, namely propane, butane, isobutane, pentane, isopentane, neopentane, and cyclopentane, are selected for the two cycles. At the design system parameters, the highest work 48.71 kW, is obtained by the split cycle with butane. For most of fluids, the split cycle has a higher work than the dual pressure cycle. Furthermore, with the increase of turbine inlet pressure, net work of the split cycle goes up firstly and then decreases, while the work of dual pressure cycle increases slowly. For the split cycle, there exists a split ratio to get the maximum network. However, for the dual pressure cycle, the larger the evaporation temperature, the higher the net work. On this basis, system parameters are optimized by genetic algorithm to maximize net work. The results indicate that the highest work 49.96 kW of split cycle is obtained by pentane. For the considered fluids, except cyclopentane, split cycle always has a higher work than dual pressure cycle. Due to the higher net work and fewer system components, split cycle is recommended for the engine waste heat recovery.

Keywords: split cycle; dual pressure cycle; thermodynamic analysis; waste heat recovery



Citation: Lin, X.; Chen, C.; Yu, A.; Yin, L.; Su, W. Performance Comparison of Advanced Transcritical Power Cycles with High-Temperature Working Fluids for the Engine Waste Heat Recovery. *Energies* **2021**, *14*, 5886. <https://doi.org/10.3390/en14185886>

Academic Editor: Andrea De Pascale

Received: 30 July 2021

Accepted: 16 September 2021

Published: 17 September 2021

Publisher's Note: MDPI stays neutral with regard to jurisdictional claims in published maps and institutional affiliations.



Copyright: © 2021 by the authors. Licensee MDPI, Basel, Switzerland. This article is an open access article distributed under the terms and conditions of the Creative Commons Attribution (CC BY) license (<https://creativecommons.org/licenses/by/4.0/>).

1. Introduction

1.1. Background

With the growth of economy and population, countries around the world are facing serious energy shortages. As one of the main driven devices for global transportation, the energy consumption of the internal combustion engine (ICE) accounts for 30% of the transportation field. However, so far, the ICE efficiency is still relatively low, only about 30–40% [1]. For the remaining energy, two-thirds are directly discharged in the form of exhaust gas, and the other one-third is transferred to the cooling water. Therefore, how to improve the ICE efficiency and reduce the fossil fuel consumption has become a subject with extensive research [2]. Nowadays, in order to improve the efficiency of ICE, researchers are working on conventional diesel combustion to develop innovative combustion systems, which are able to reduce the CO₂ emission, and improve the NO_x-Soot trade-offs. Many technologies, such as specific fuel injection system [3], waste heat recovery [4] and dual-fuel combustion by using alternative fuels [5] have been proposed. Among these technologies, waste heat recovery has attracted much attention. For the efficient heat recovery of ICE, organic Rankine cycle (ORC) as a promising method has been widely employed [4]. This is due to its simple structure, reliable operation and easy maintenance [6]. Furthermore, ORC has less influence on the back pressure of engine and can be arranged in a narrow and closed vehicle environment.

1.2. Organic Rankine Cycles

In general, ORCs can be classified into the subcritical ORC and transcritical ORC, depending on whether the operating temperature and pressure are above the critical parameters of working fluids or not. For the subcritical ORC, the evaporation temperature is usually low, and the cycle is generally suitable for low-temperature heat sources. At present, in terms of ICE applications, subcritical ORC has been theoretically and experimentally studied. For instance, aiming at the large temperature and mass flow variations in the ICE waste gas, researchers from University of Liege and Politecnico di Milano proposed a multiple model predictive controller for recovery of ORC, and experimentally applied the model to maximize the output power of a 11 kW small-scale ORC [7]. Similarly, to recover the waste heat from a heavy-duty diesel engine, Peralez et al. [8] in the University of Lyon developed a gain-scheduled PID strategy to regulate the superheating temperature. The corresponding experimental results illustrated the enhanced performance under the disturbance of exhaust gas. Furthermore, Zhang et al. [9] from Beijing University of Technology established an ORC experimental system. When the diesel engine output power was 250 kW, the maximum power output of ORC was 10.38 kW, and the maximum ORC efficiency and overall system efficiency were 6.48% and 43.8%, respectively. However, the point that cannot be overlooked is that the temperature of exhaust gas is typically above 500 °C [10], and there exists a large temperature difference between the organic working fluid and the exhaust gas for the subcritical cycle. Thus, to improve the system efficiency, much effort has been devoted to modifying the cycle configurations.

As for the transcritical ORC, the working fluid extracts the waste heat of engine at supercritical state. Due to the fact that the phase change of working fluid does not exist, the temperature of working fluid can be better matched with that of waste gas. In general, the transcritical ORC has higher thermal and exergy efficiencies than the subcritical cycle [11]. Thus far, a few studies have been conducted to apply transcritical ORC to the waste heat recovery in ICE. As an example, Yang [12] from National Kaohsiung Marine University employed the transcritical ORC to recover the waste heat from four sources: exhaust gas, cylinder cooling water, scavenge air cooling water and lubricating oil of a marine diesel engine. Different working fluids were employed to analyze the system performance. Thereafter, the author [13] proposed an economic evaluation method for the waste heat recovery by simultaneously considering thermal efficiency and working pressure ratio. It was found that R1234yf has a higher economic efficiency. However, it should be pointed out that in the waste heat recovery of ICE, the transcritical ORC still faces two severe challenges: one is that the classical configurations usually have an insufficient capacity to recover the waste heat, thus making the waste gas still have a relatively high temperature at the outlet of thermodynamic system. Another is that the commonly used working fluids are highly possible to decompose at higher temperatures and pressures of transcritical cycle. Thus, aiming at the above challenges, various cycle layouts have been developed, and high-temperature fluids are considered.

1.3. Cycle Configurations

Based on the simple configurations of subcritical and transcritical ORC, various cycle configurations have been proposed and designed to deeply recover the waste heat and greatly improve the energy conversion efficiency [14]. In general, these configurations can be divided into four groups, as illustrated in Table 1. The first group is called recuperative cycle, in which a recuperator is added to transfer heat from low-pressure turbine outlet stream to high-pressure liquid stream. Before the recuperator, the engine coolant is usually employed to preheat the liquid stream [15]. The second is the split cycle. It's proposed to further decrease the waste gas outlet temperature, based on recuperative cycle [16]. For the split cycle, the high pressure fluid is divided into two streams. One stream enters the recuperator, while the other stream directly extracts the waste heat at low temperatures. After that, these two streams are mixed and continuously absorb the waste heat at high temperatures.

Table 1. Four groups of cycle configurations.

Cycle	Schematic Diagram of the Cycle
Recuperative cycle	
Split cycle	
Combined cycle	
Dual pressure cycle	

The third group is the combined cycle [17]. It means that this configuration consists of a high-temperature cycle (HT cycle) and a low-temperature cycle (LT cycle). These two cycles both have compression, heating, expansion and condensation processes and can operate separately. The HT cycle is mainly employed for the waste heat recovery of engine, while the LT cycle can be powered by the residual heat of exhaust gas, engine coolant, and the rejected condensation heat of HT cycle. Theoretically, there is no limit on the types of HT cycle. Besides the commonly used ORC, considering the advantages of compact system and high efficiency [1], supercritical CO₂ (S-CO₂) power cycle is often used as the HT cycle. For instance, the group of Markides in Imperial College of London [18] presented an S-CO₂-ORC combination cycle. The ORC can recover heat rejected from the S-CO₂ cycle, as well as thermal energy available from the jacket-water and exhaust-gas streams that have not been utilized by the S-CO₂ cycle. The optimization results showed that system can deliver a maximum net power output of 215 kW at a cost of 4670 \$/kW, which are 58% and 4% higher than those of the standalone S-CO₂ cycle, respectively. Meanwhile, Battista et al. [19] from University of L'Aquila combined S-CO₂ cycle with the R1233zde Rankine cycle. It was reported that the combined cycle can realize an overall net efficiency 3–4% higher than that of a single ORC in the application of ICE waste heat recovery. If ORC is employed to both cycles, there usually exist four different configurations of cascade cycle, namely subcritical–subcritical cycle, subcritical–transcritical cycle, transcritical–subcritical cycle, and transcritical–transcritical cycle. For the ORC structure, it can be recuperative, split or other advanced layouts.

The last group is the dual pressure cycle [20]. The aim of this cycle is to avoid the irreversible loss generated in the heat transfer process between the HT cycle and the LT cycle. In order to reduce the system cost and improve the compactness, the condenser is usually shared by these two cycles. Being different with the combined cycle, the dual-pressure cycle employs the same working fluid in the HT and LT cycles. Thus, only organic fluids are considered here. For the dual pressure cycle, HT cycle usually operates at the transcritical condition, while the LT cycle belongs to the subcritical system. In order to obtain the system performance for the heat recovery of heavy-duty truck diesel engine, Chen et al. established the corresponding thermodynamic model with cyclopentane as the working fluid. The results revealed that the engine peak thermal efficiency can be improved from 45.3% to 49.5%, where the brake specific fuel consumption decreases from 185.6 g/(kW·h) to 169.9 g/(kW·h).

In fact, the above configurations have been summarized by Liu et al. [21] to illustrate the cycle development for diesel engine waste heat recovery. The interest readers can refer to this literature [21]. Furthermore, it should be pointed out that in the existing analysis on these configurations, a relatively low condensation temperature (≤ 30 °C) is usually presumed, and the engine coolant is always employed to preheat or evaporate the working fluid [21]. This operating condition may be attainable for a stationary engine. However, for a mobile engine, due to the lack of cooling water, how to effectively condense the working fluid has to be considered. In general, there are three ways to reject the condensation heat, according to the carried heat fluid, namely air, medium fluid and engine coolant [22]. Under this condition, the condensation temperature has to be increased, even up to 90 °C. Thus, the engine coolant is no longer suitable to be a heat source. It's more practical to effectively recover the waste heat of exhaust gas. Furthermore, for the above configurations, little work has been conducted to compare and optimize the corresponding performances under practical conditions of mobile engine.

1.4. Working Fluids

Besides the cycle configurations, the performance of waste heat recovery is also strongly related with the working fluids. In general, working fluids can be classified into low-temperature fluids and high-temperature fluids, according to the thermal decomposition temperature. For commonly used working fluids, most of them belong to low-temperature fluids, and the thermal decomposition temperatures are generally around

300 °C [23], thus limiting the highest operation temperature of thermodynamic system. By considering the fluid decomposition, Benato et al. analyzed the transient performance of ORC under different heat loads [24]. In order to avoid the thermal decomposition of these low-temperature fluids, an intermediate heat transfer fluid is usually employed to transport the waste heat to the ORC. For example, Wang et al. [25] used thermal oil to decrease the heat source temperature of ORC from around 500 °C to about 200 °C, which is a safe temperature for organic fluids. In addition, the experimental research of Shu et al. [26] proved that thermal oil has a large inertia to the change of heat source, and is suitable for the unstable conditions of the engine.

For the high-temperature fluids, they mainly include alkanes, aromatics, siloxanes and alcohols, as summarized by the review literature [4]. These fluids have been widely used in the recovery of high-temperature waste heat. For instance, Shu et al. [27] applied ten alkanes into subcritical simple ORCs for engine waste heat recovery at the temperature 519 °C, and six indicators, including thermal efficiency, exergy destruction factor, turbine size parameter, total exergy destruction rate, turbine volume flow ratio and net power output per unit mass flow rate of exhaust were considered to evaluate the performance of alkanes. It was concluded that the most suitable fluids were cyclohexane and cyclopentane with relatively high power output and low irreversibility. Furthermore, aiming at the waste heat recovery of heavy trucks, Grelet et al. [22] considered different condensation modes of subcritical simple ORC and employed ethanol as working fluid, because of its high net power output. For various configurations including split cycle, combined cycle and dual-pressure cycle, Liu et al. [21] employed cyclopentane into these configurations to recover the waste heat of diesel engine at the temperature 517.3 °C. However, in their calculations, the condensation temperature was only set to be 35 °C, and the condensation pressure was far lower than 1 bar. Besides the high-temperature organic fluids, water is also considered in the HT cycle of cascade configuration. To recover the exhaust heat at temperature 519.00 °C, Shu et al. [28] investigated various combined cycles. R143a was used as the working fluids for the LT cycle (transcritical configuration), while the water and siloxane were, respectively, applied in the HT cycle. It should be noted that a large footprint is usually required for the system with water. This hinders the application of water system in the narrow car space. Furthermore, as a nature fluid, CO₂ is also widely considered in transcritical cycles to recover the high temperature waste heat of engines [29]. However, due to the low critical temperature ($T_c = 30.98$ °C) and high critical pressure ($P_c = 7.34$ MPa) of CO₂, transcritical CO₂ cycle faces the high operation pressure and condensation difficulty for the heat recovery of mobile engine [30]. From the above reviews, it can be concluded that for a mobile engine, CO₂ and water power cycles still face great challenges to recover the waste heat. In practical applications, high-temperature organic fluids are usually preferred. However, in the existing studies, only certain fluids are considered for a specified cycle configuration. Few work focus on the performance comparison of different high-temperature fluids in advanced cycles.

1.5. Work's Aim

Aiming at above issues, two advanced cycles, namely split cycle and dual pressure cycle, are employed to recover the high-temperature waste heat of mobile engine. Mathematic models are established to obtain the cycle performance, and a genetic algorithm (GA) is employed to optimize the key system parameters with the goal to maximize the net work. Thereafter, according to the condition of exhaust gas, working fluids are screened from the high-temperature fluids. The aim of this work is listed as follows:

- Analyze and compare the performances of split cycle and dual pressure cycle for different high-temperature working fluids.
- Investigate the effects of turbine inlet temperature and pressure, split ratio, evaporation temperature on the system performances for the split cycle and dual pressure cycle. Conduct the sensitivity analysis of turbomachinery efficiency and obtain the system performance under different condensation modes.

- Optimize the system parameters of the considered two cycles to obtain the corresponding maximum net works, and conduct the performance comparison.

2. Cycle Layouts

To effectively recover the high temperature waste heat of engine and improve the temperature match between the exhaust gas and the working fluid, a transcritical power cycle is employed and a recuperator is also considered to recuperate the fluid heat at the turbine outlet, as shown in Figure 1. Take pentane as a working fluid, Figure 2 presents the corresponding T-s diagram. Furthermore, under design conditions, the outlet gas temperature and heat recovery efficiency of recuperative cycle are calculated for different high-temperature working fluids, as illustrated in Figure 3. It can be seen that at the inlet gas temperature 600 °C, the recuperative cycle can reduce the gas temperature to around 250 °C, and the corresponding heat recovery efficiency is around 60%. The relatively high outlet gas temperature is caused by the fact that a large amount of heat is recuperated in the recuperator, thus increasing the working fluid temperature at the inlet of heater.

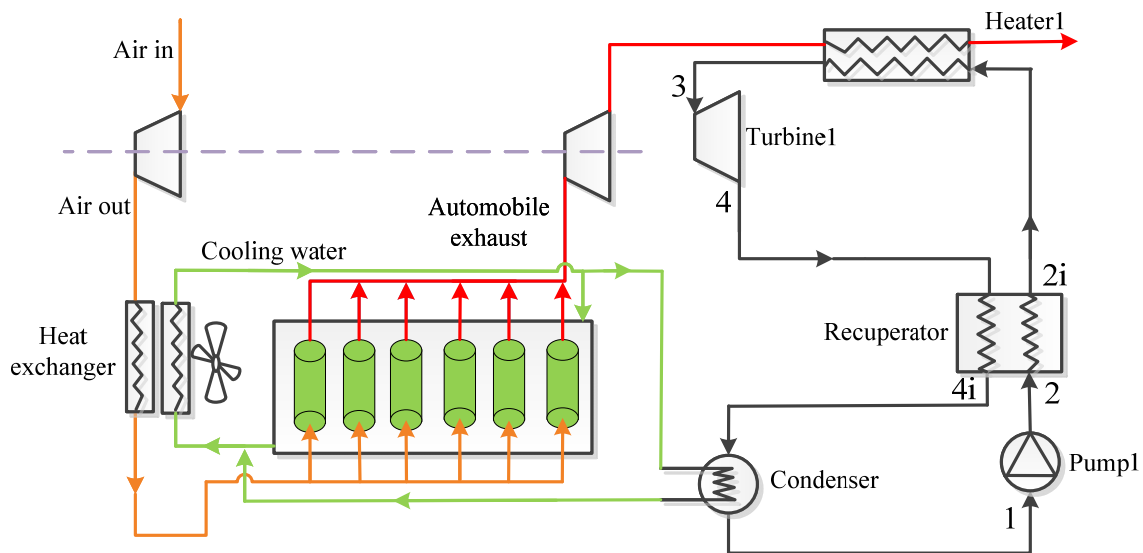


Figure 1. Systematic diagram of the recuperative cycle.

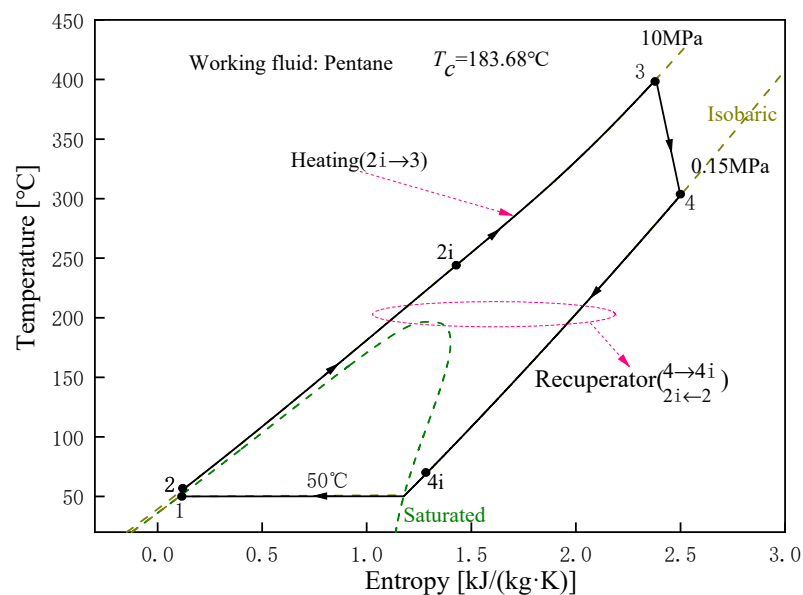


Figure 2. T-s diagram of the recuperative cycle with pentane under design conditions.

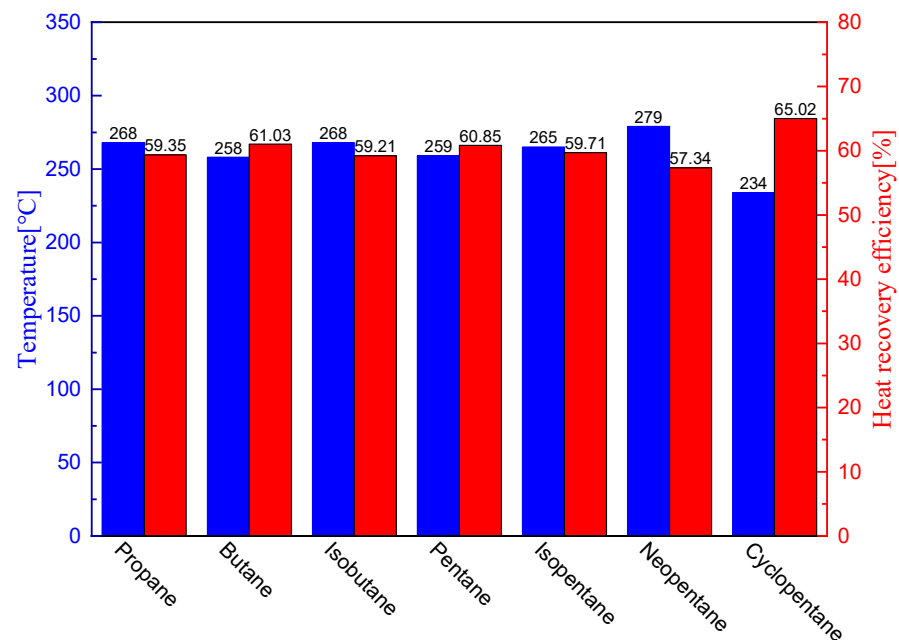


Figure 3. Waste heat recovery of recuperative cycle under design conditions.

Aiming at this phenomenon, a split cycle is employed to further reduce the waste gas temperature, as shown in Figures 4 and 5. The corresponding working process of split cycle is described as follows: the total flow at the pump outlet is split into two streams. The first stream flows into the recuperator and exchanges heat with the hot fluid at the turbine outlet to state point 2i. The second stream in Heater2 absorbs heat from the outlet exhaust gas of Heater1. Thereafter, the two flows are mixed and heated to state point 3 in Heater1 by the high temperature exhaust gas discharged from the ICE. Subsequently, the heated working fluid enters the turbine and produces work in expansion process 3–4. The exhaust stream after passing through the turbine transfers heat to the first stream in the recuperator, and is cooled to state point 4i. After that, the fluid vapor is condensed to a saturated liquid state in the condenser. To complete the cycle, the condensed liquid is compressed by the pump. By introducing Heater2, the split cycle can deeply extract the waste heat and output more work compared to the recuperative cycle. Furthermore, by splitting the flow, the heat capacity difference between the hot and cold flows in the recuperator can be reduced, so that the temperature match of the recuperator can be improved.

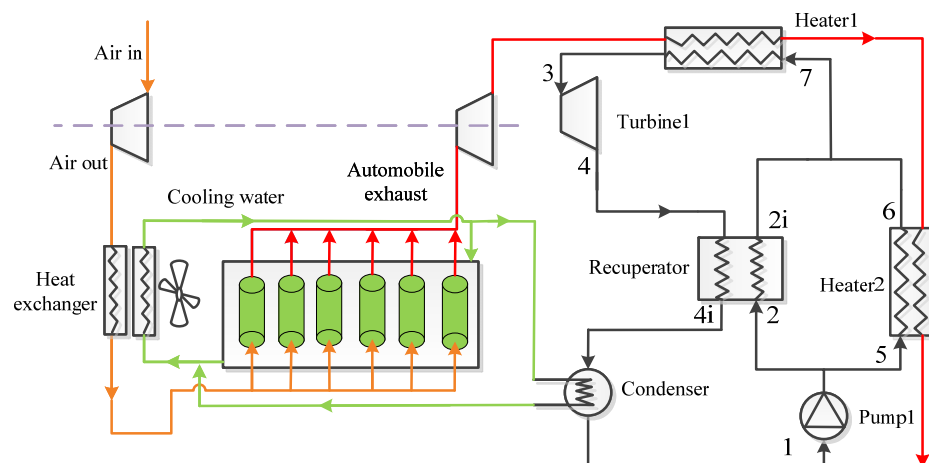


Figure 4. Systematic diagram of the split cycle.

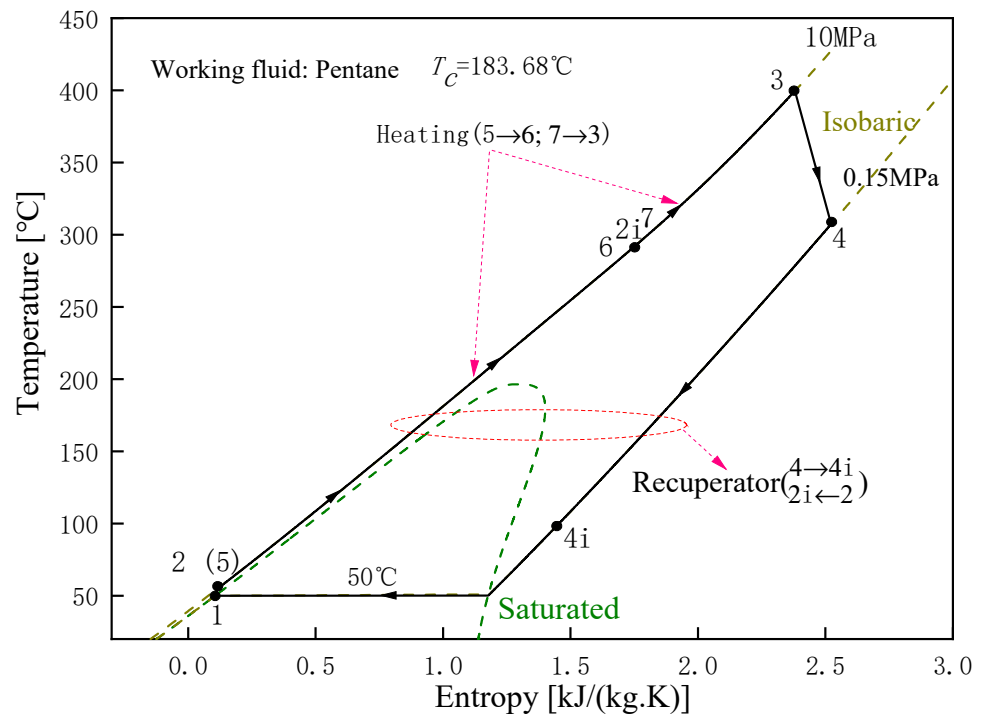


Figure 5. T-s diagram of the split cycle with pentane under design conditions.

Besides the above transcritical power cycles, cascade cycle and dual pressure cycle are also widely employed in the high-temperature waste heat recovery. Considering the fact that the complex structure of cascade cycle is difficult to be reasonably arranged in a narrow and closed vehicle environment, only the dual pressure cycle is investigated here. The system structure and T-s diagram are, respectively, given in Figures 6 and 7. It can be seen that on the basis of the recuperative cycle, another subcritical cycle is introduced to extract the residual waste heat. Furthermore, there exist two pumps to supply different high pressures for the two cycles. After expansion in the turbine, the fluids from these cycles are mixed and condensed.

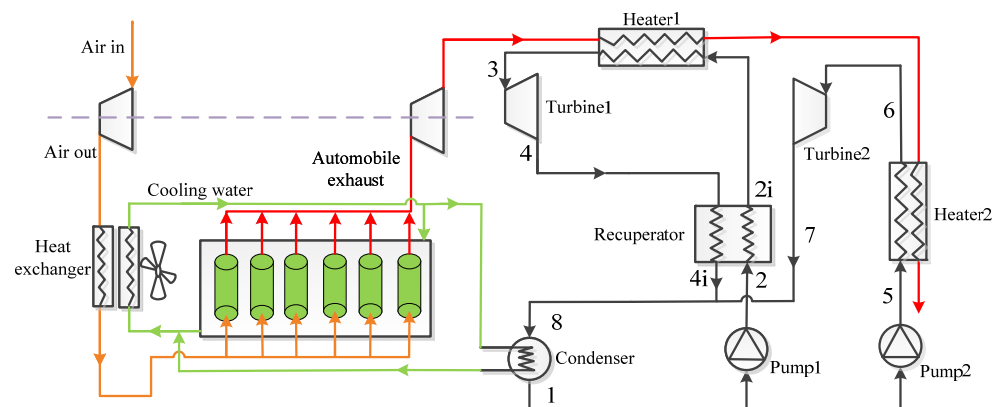


Figure 6. Systematic diagram of the dual pressure cycle.

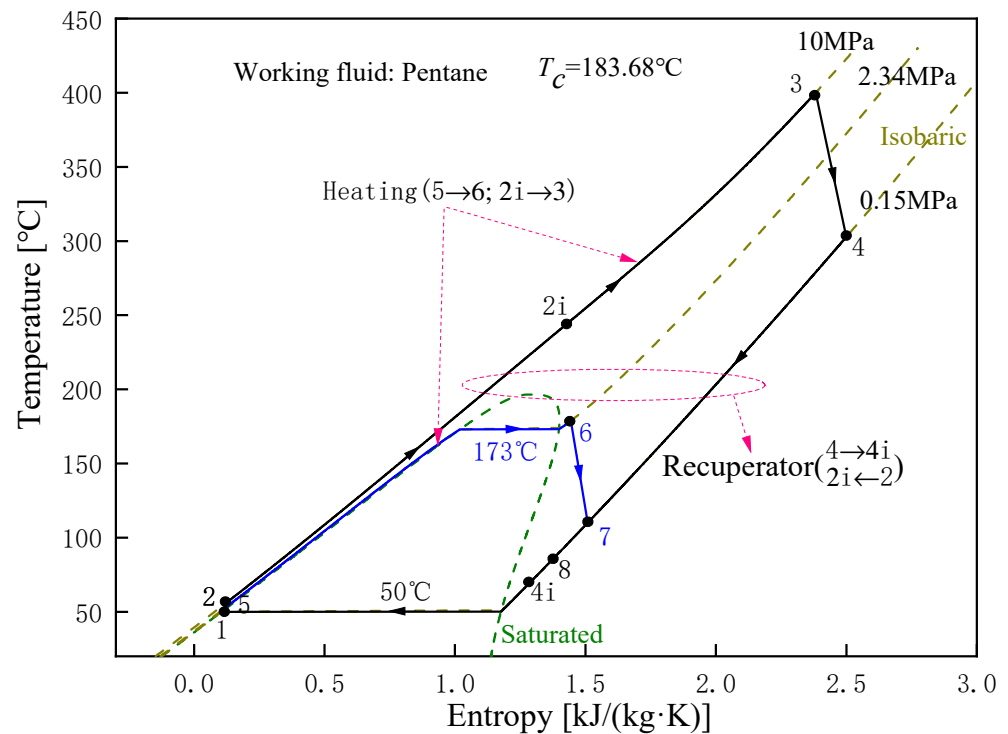


Figure 7. T-s diagram of the dual pressure cycle with pentane under design conditions.

It should be noted that in the above cycles, the working fluid is always condensed by the engine coolant, so that the condensation heat can be finally rejected by the engine radiator. In fact, there are two other methods to condense the working fluid. One is that the working fluid is directly cooled by the air. Another is that the fluid is condensed by an intermediate medium, such as ethanol and water. For different condensation methods, different condensation temperatures can be obtained. In general, the temperature varies from 30 °C to 90 °C [22].

3. Thermodynamic Modeling and Optimization

3.1. Thermodynamic Modeling

To facilitate the mathematical modeling of split cycle and dual pressure cycle, the following hypotheses are made:

- The system operates in a steady-state, and working fluid has no change in kinetic energy and potential energy.
- No heat losses from system components and pipelines.
- No pressure drops in the heater, condenser or pipelines.

Based on the first and second laws of thermodynamics, system components including heat exchangers and turbomachineries are, respectively, modeled. The employed equations for split cycle and dual pressure cycle are summarized in Tables 2 and 3, respectively. Considering that these equations have been widely used to model the transcritical power cycles, detailed descriptions are omitted. The interest readers can refer to the references [31,32].

Table 2. Thermodynamic model of each component for split cycle.

Components	Energy Models	Exergy Destruction
Heater1	$Q_{H1} = m_g(h_{g,in} - h_{g,mid}) = m_f(h_3 - h_7);$ $T_{g,mid} = T_7 + PPTD_{H1}$	$I_{H1} = E_{g,in} - E_{g,mid} - E_3 + E_7$
Turbine1	$W_{T1} = m_f(h_3 - h_4) = m_f(h_3 - h_{4s})\eta_t$	$I_{T1} = E_3 - E_4 - W_{T1}$
Recuperator	$Q_R = m_f(h_4 - h_{4i}) = m_f(h_{2i} - h_2) \times SR$ $T_{4,pp} = T_{2,pp} + PPTD_R$	$I_R = E_4 - E_{4i} + E_2 - E_{2i}$
Heater2	$Q_{H2} = m_g(h_{g,mid} - h_{g,out}) = m_f(1 - SR)(h_6 - h_5)$ $SR \times h_{2i} + (1 - SR)h_6 = h_7$ $T_{56,pp} = T_{g,pp} + PPTD_{H2}$	$I_{H2} = E_5 - E_6 + E_{g,mid} - E_{g,out}$
Condenser	$Q_C = m_f(h_{4i} - h_1)$	$I_C = E_{4i} - E_1 - Q_C(1 - T_0/T_{av1})$
Pump1	$W_{P1} = m_f(h_2 - h_1) = m_f(h_{2s} - h_1)/\eta_p$	$I_{P1} = E_1 - E_2 + W_{P1}$

Table 3. Thermodynamic model of each component for dual pressure cycle.

Components	Energy Models	Exergy Destruction
Heater1	$Q_{H1} = m_g(h_{g,in} - h_{g,mid}) = m_{f1}(h_3 - h_{2i});$ $T_{g,mid} = T_{2i} + PPTD_{H1}$	$I_{H1} = E_{g,in} - E_{g,mid} - E_3 + E_{2i}$
Turbine1	$W_{T1} = m_{f1}(h_3 - h_4) = m_{f1}(h_3 - h_{4s})\eta_t$	$I_{T1} = E_3 - E_4 - W_{T1}$
Recuperator	$Q_R = m_{f1}(h_4 - h_{4i}) = m_{f1}(h_{2i} - h_2)$ $T_{4i} = T_2 + PPTD_R$	$I_R = E_4 - E_{4i} + E_2 - E_{2i}$
Heater2	$Q_{H2} = m_g(h_{g,mid} - h_{g,out}) = m_{f2}(h_6 - h_5)$ $T_{56,pp} = T_{g,pp} + PPTD_{H2}$	$I_{H2} = E_5 - E_6 + E_{g,mid} - E_{g,out}$
Turbine2	$W_{T2} = m_{f2}(h_6 - h_7) = m_{f2}(h_6 - h_{7s})\eta_t$	$I_{T2} = E_6 - E_7 - W_{T2}$
Condenser	$Q_C = (m_{f1} + m_{f2})(h_8 - h_1)$ $m_{f1} \times h_{4i} + m_{f2}h_8 = (m_{f1} + m_{f2})h_8$	$I_C = E_8 - E_1 - Q_C(1 - T_0/T_{av1})$
Pump1	$W_{P1} = m_{f1}(h_2 - h_1) = m_{f1}(h_{2s} - h_1)/\eta_p$	$I_{P1} = E_1 - E_2 + W_{P1}$
Pump2	$W_{P2} = m_{f2}(h_5 - h_1) = m_{f2}(h_{5s} - h_1)/\eta_p$	$I_{P2} = E_5 - E_1 + W_{P2}$

For heat exchangers such as heater and recuperator, besides the constraint of energy conservation, the pinch point temperature difference (PPTD) is usually applied to assure the occurrence of heat exchange. Due to the fact that PPTD in heat exchangers is closely related with the total heat capacity of fluid on both sides, under a given value of PPTD, the corresponding location is usually determined by iteration. For example, in the recuperator modeling of split cycle, since mass flow rates in two sides of recuperator are not equal, PPTD may not be located at the end of recuperator. Thus, temperature at point 4i is first assumed. Then, based on the energy balance of recuperator, temperatures are determined to calculate the PPTD. Finally, the temperature at point 4i is iterated to make the PPTD be the set value. As for the involved pumps and turbines, the operation performance is characterized by the isentropic efficiency, as illustrated in Tables 2 and 3.

Besides the energy equations, the exergy equations are also summarized in Tables 2 and 3. For these equations, the required exergy value can be determined by

$$E_i = m_i[h_i - h_0 - T_0(s_i - s_0)] \quad (1)$$

where 0 means the ambient condition. The corresponding temperature and pressure are, respectively, 25 °C and 101.3 kPa. Special care should be given to the condenser. In the irreversibility calculation, the average temperature of cooling medium is set to be the average temperature of working fluid minus 20 °C.

Based on the calculations in Tables 2 and 3, the net work can be calculated by

$$W_{net} = \begin{cases} W_{T1} - W_{P1} & \text{Split cycle} \\ W_{T1} + W_{T2} - W_{P1} - W_{P2} & \text{Dual pressure cycle} \end{cases} \quad (2)$$

Thermal efficiency is defined as

$$\eta_{th} = \frac{W_{net}}{Q_{H1} + Q_{H2}} \quad (3)$$

In order to measure the extent to which waste heat from exhaust gas is recovered, the recovery efficiency is employed, as given by Equation (4).

$$\eta_{re} = \frac{Q_{H1} + Q_{H2}}{m_g(h_{g,in} - h_{g,out}(T = 25^\circ\text{C}))} \times 100\% \quad (4)$$

Besides the above energy efficiencies, the exergy efficiency is obtained by

$$\eta_{ex} = \frac{W_{net}}{E_{g,in} - E_{g,out}} \times 100\% \quad (5)$$

Furthermore, it should be noted that SR is employed in the split cycle, due to the fact that SR is required in the modeling of recuperator and Heater2. SR can be independently varied to regulate the heat exchange in recuperator and Heater2. However, for the dual pressure cycle, considering that there exist two subcycles, m_{f1} and m_{f2} are used to denote the mass flow rates of Turbine1 and Turbine2, respectively. Instead of SR, an evaporation temperature is given. The corresponding values are determined by the inlet temperatures of Turbine1 and Turbine2.

3.2. GA Optimization

Based on the above thermodynamic models, system parameters are optimized to get the optimal cycle performances by the employment of GA. In fact, GA is designed and proposed based on the evolution laws of organisms in nature. It is a computational model of biological evolutionary process that simulates the natural selection and genetic mechanism of Darwinian evolutionary theory [33]. Nowadays, because of its simplicity, versatility, and suitability for parallel processing, GA has been widely used to optimize thermal systems such as ORC [34,35], refrigeration cycle [36,37] and S-CO₂ Brayton cycle [1,38]. In this work, for the waste heat recovery of exhaust gas, the highest operation temperature and pressure, the mass ratio of split cycle and the evaporation temperature of dual pressure cycle are optimized to maximize the net work. The corresponding flowchart of GA is illustrated in Figure 8. GA first encodes the randomly generated initial population chromosomes, which are later decoded to obtain the corresponding system parameters. Under the given exhaust gas conditions, the obtained system parameters are substituted into the established models for thermodynamic calculations. The net work is used as a fitness function for each chromosome. Then, PPTDs of heaters and recuperator are checked. If the PPTD is less than the minimum value, the fitness of corresponding chromosome is set to zero. Thereafter, based on the sorting of fitness function, offspring are reproduced by genetic operations such as selection, crossover and mutation. All chromosomes will be replaced by these offspring, and the net work is recalculated. The optimization will end when the genetic calculation is iterated to the maximum number of generation. Finally, the optimal parameters in the final population are substituted into the thermodynamic calculations to obtain system efficiency, recovery efficiency and other parameters. For the thermodynamic cycle calculation, the flow diagrams of split cycle and dual pressure cycle are presented in Figures 9 and 10, respectively. It can be seen that in the calculation of split cycle, numerical iteration is used to determine temperatures of recuperator and heaters. This is because that mass flow rates in both sides of the recuperator are not equal with each other, thus resulting into the difficulty of determining the pinch point. However, in the calculation of dual pressure cycle, under given inlet temperature of Turbine1 and evaporation temperature, parameters of each sub-cycle are easily determined. Considering the fact that there are equal mass flow rates in both sides of recuperator, iterations are not required.

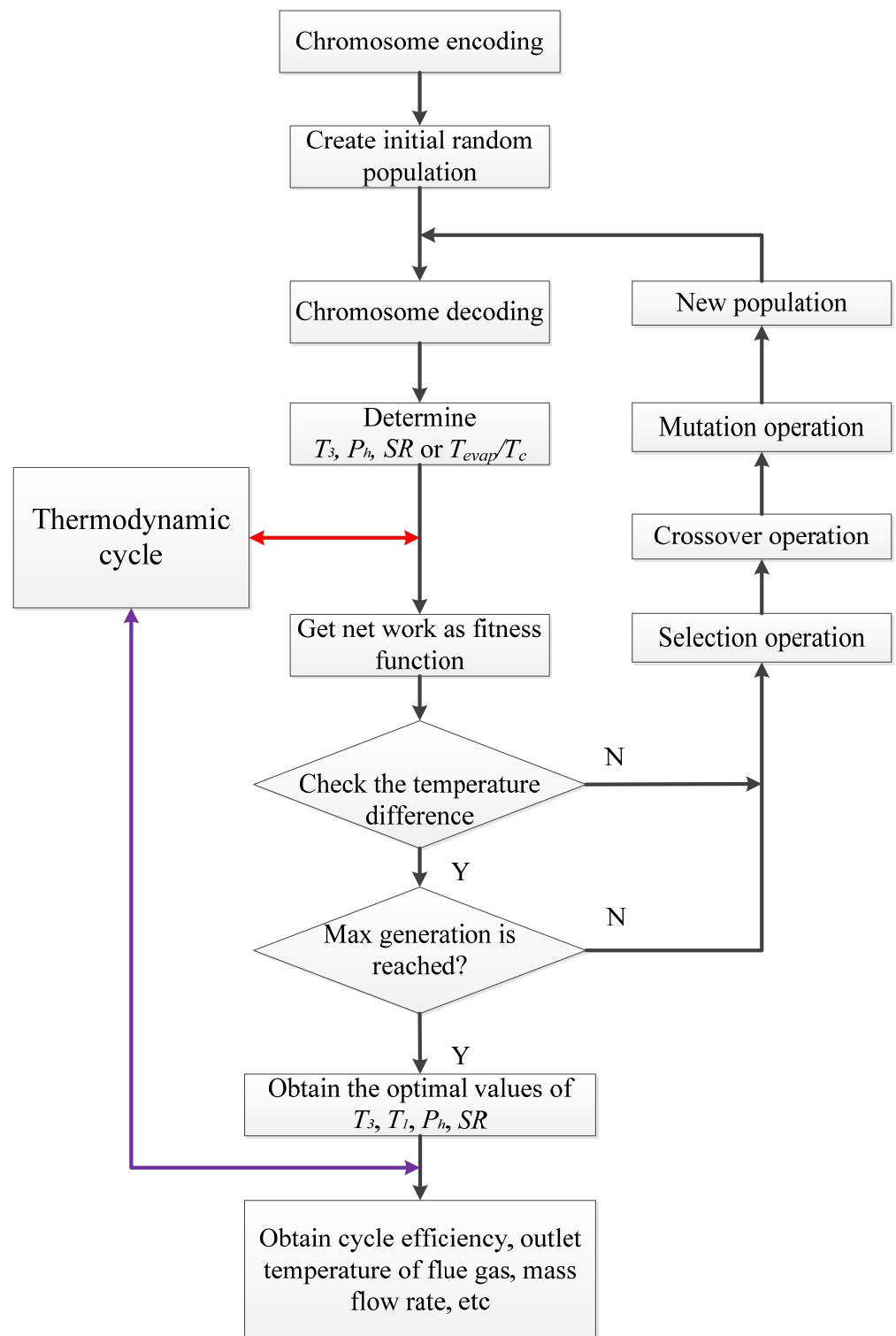


Figure 8. Flow diagram of GA for the system parameter optimization.

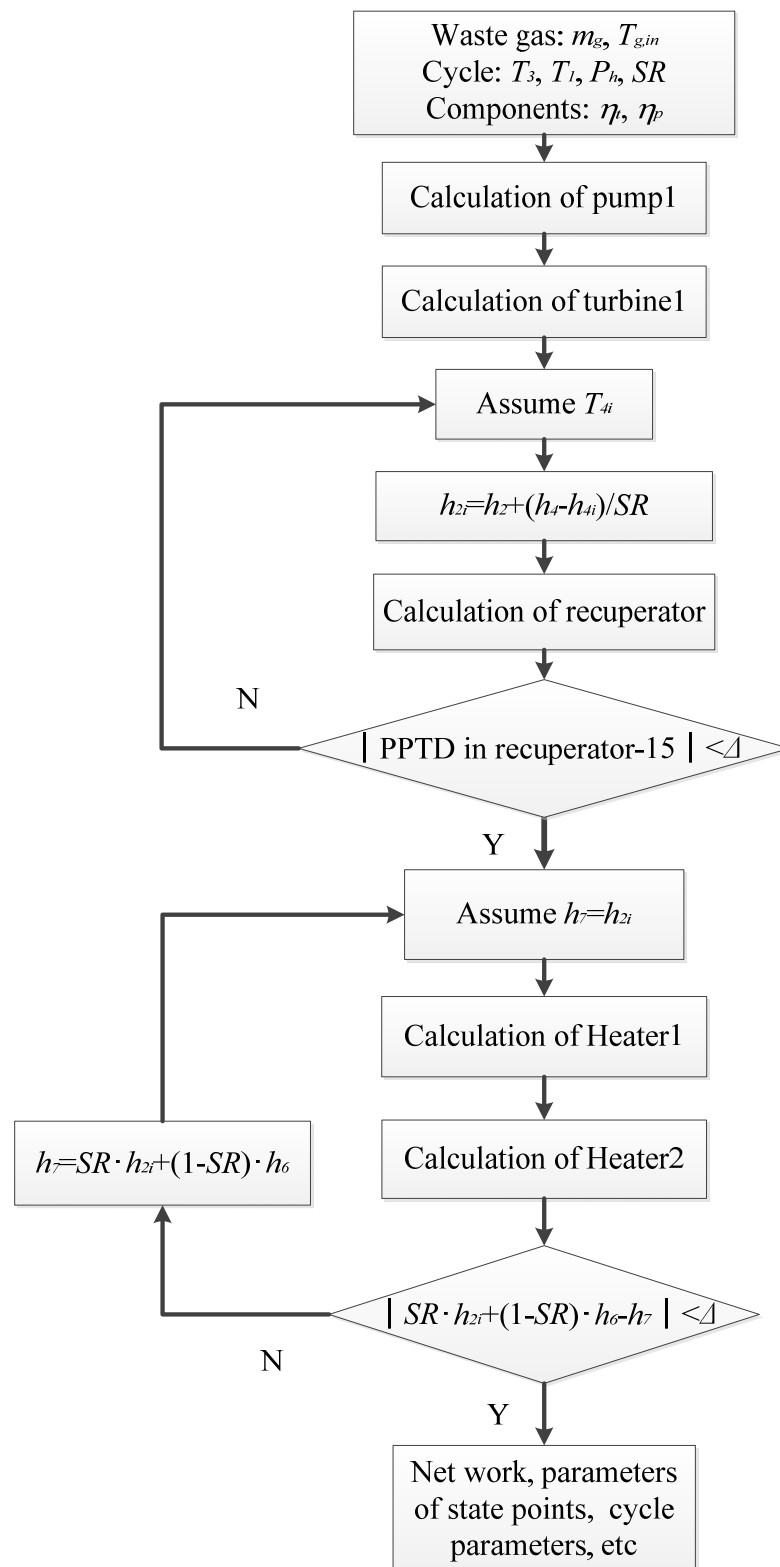


Figure 9. Thermodynamic calculation routine of the split cycle.

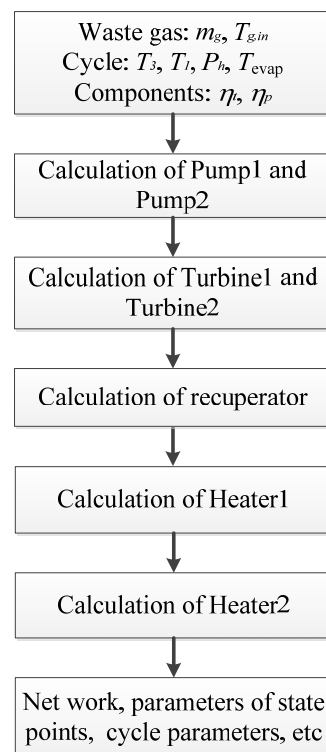


Figure 10. Thermodynamic calculation routine of the dual pressure cycle.

In GA optimization, operators are selected based on normalized geometric distributions; crossover performs an interpolation along the line formed by two parents; and a parameter of the parent is mutated under a non-uniform probability distribution. In addition, the population size and maximum generation are set to 100 and 80, respectively.

4. Cycle Conditions and Potential Working Fluids

This study uses a turbocharged and inter-cooled diesel engine with 6-cylinder common rail. The engine is employed to drive the road roller, which works very stable. According to the experimental measurements on the road roller, the corresponding ICE parameters are listed in Table 4. For the exhaust gas compositions, only four components, namely CO₂, H₂O, N₂ and O₂ are considered, and the remaining nitrogen oxides and sulfur oxides, which account for very low proportions, are not considered.

Table 4. Main parameters and exhaust gas components of ICE.

Parameters	Values	Gas Components	Mass Fraction (%)
Power output	258 kW	CO ₂	12.06
Engine displacement	8.9 L	H ₂ O	1.91
Input temperature of exhaust gas	600 °C	N ₂	75.45
Mass flow of exhaust gas	0.3250 kg/s	O ₂	10.58
Exhaust gas pressure	0.1 MPa		

In order to employ the split cycle and the dual pressure cycle to effectively recover the waste heat, appropriate working fluids have to be screened. For the 600 °C waste gas, high-temperature working fluids are considered. By reviewing the literature, 32 commonly used working fluids for high-temperature heat source are summarized in Appendix A. Considering the fact that the condensation pressure should be larger than 0.1 Mpa, only seven working fluids, namely propane, butane, isobutane, pentane, isopentane, neopentane, cyclopentane, are finally selected, as presented in Table 5. The physical parameters of these working fluids are summarized in Table. For the seven working fluids, system parameters

are designed for the split and dual pressure cycles, as shown in Table 6. It can be observed that under design conditions, the setting values for the inlet temperature and pressure of turbine1 are 400 °C and 10 MPa, respectively. The condensation temperature is designed as 50 °C. For SR of split cycle, it is possible to artificially adjust the cycle parameters to suit the split ratio. Therefore, SR is set to 0.7 under design conditions. For the dual pressure cycle, evaporation temperature of subcritical cycle is set to $0.95 T_c$, which directly determines the inlet temperature and pressure of Turbine2. Furthermore, for both cycles, PPTDs in Heater1, Heater2 and the recuperator are 15 °C. The isentropic efficiencies of both the pump and the turbine are 0.75.

Table 5. Basic thermodynamic properties of the selected fluids.

Working Fluid	T_c (°C)	P_c (kPa)	Condensation Pressure (kPa)		
			30 °C	50 °C	90 °C
Propane	96.74	4251.20	1079.00	1713.30	3764.10
Butane	151.98	3796.00	283.41	495.75	1249.30
Isobutane	134.66	3629.00	404.72	684.90	1642.00
Pentane	196.55	3370.00	81.99	159.25	470.34
Isopentane	187.20	3378.00	109.17	205.51	578.61
Neopentane	160.59	3196.00	200.57	355.80	913.23
Cyclopentane	238.57	4571.20	51.36	103.83	326.33

Table 6. Standard design conditions and parameter ranges for split and dual pressure cycles.

Design Parameters	Set Value	Range of Variation
Turbine inlet temperature T_3	400 °C	300~550 °C
Turbine inlet pressure P_3	10 MPa	5~15 MPa
Condensation temperature T_1	50 °C	30 °C, 50 °C, 70 °C, 90 °C
SR for split cycle	0.7	0~1
Evaporation temperature for dual pressure cycle	$0.95 T_c$	$0.75 T_c$ ~ $0.95 T_c$
Superheat temperature for dual pressure cycle	5 °C	—
PPTD in Heater1	15 °C	—
PPTD in Heater2	15 °C	—
PPTD in recuperator	15 °C	—
Pump efficiency	0.8	0.5~0.9
Turbine efficiency	0.7	0.5~0.9

To better evaluate the two cycles, sensitivity analyses are carried out on the turbine inlet temperature and pressure, the condensation temperature, the split ratio of split cycle, and the evaporation temperature of dual pressure cycle. Variation ranges of these five parameters are also shown in Table 6. For different working fluids, turbine inlet temperature (T_3) varies from 300~550 °C at an interval of 5 °C and turbine inlet pressure (P_h) varies from 5 MPa to 15 MPa at an interval of 0.5 MPa. Furthermore, the split ratio varies from 0 to 1, corresponding to a change in flow into the recuperator from 0 to m_f . As for the condensation process, considering different condensation methods, four temperatures, namely 30 °C, 50 °C, 70 °C and 90 °C, are considered. For the evaporation temperature of dual pressure cycle, the corresponding range is $0.75 T_c$ ~ $0.95 T_c$.

Under the above conditions, cycle performances of considered systems can be analyzed and optimized, based on the REFPROP calculation for the thermodynamic properties of the exhaust gas and working fluids [39]. The corresponding calculation routines of recuperative and split cycles are presented in Figures 9 and 10, respectively.

5. Results and Discussion

In this section, under design conditions, thermodynamic performances of the split cycle and dual pressure cycle are firstly analyzed and compared with each other for the given working fluids. Then, the effects of key parameters including turbine inlet

temperature (T_3) and pressure (P_3), split ratio (SR), evaporation temperature, condensation temperature and turbomachinery efficiency on the system performances are investigated. On this basis, key parameters are optimized to obtain the maximum net work by the established GA models.

5.1. Cycle Analysis and Performance Comparison under Design Conditions

Figure 11 illustrates the waste heat recovery performance of seven working fluids in the split cycle and dual pressure cycle under design conditions. Compared with the recuperative cycle in Figure 3, the two advanced cycles have the lower outlet temperatures of waste gas and higher recovery efficiencies for all fluids. Meanwhile, the dual pressure cycle has the lowest outlet temperatures of waste gas and the highest recovery efficiencies for working fluids propane, butane, isobutene, pentane, isopentane and neopentane. In the dual pressure cycle, recovery performances of these six fluids almost keep the same. The outlet temperature and heat recovery efficiency are around 66 °C and 93%, respectively. However, in the split cycle, outlet temperature of waste gas and heat recovery varies greatly with the working fluids. Among the considered working fluids, propane has the lowest gas outlet temperature 77 °C and the highest recovery efficiency 91%. Furthermore, special care should be given to cyclopentane. For both split cycle and dual pressure cycle, the cyclopentane has the highest outlet temperature and the lowest recovery efficiency.

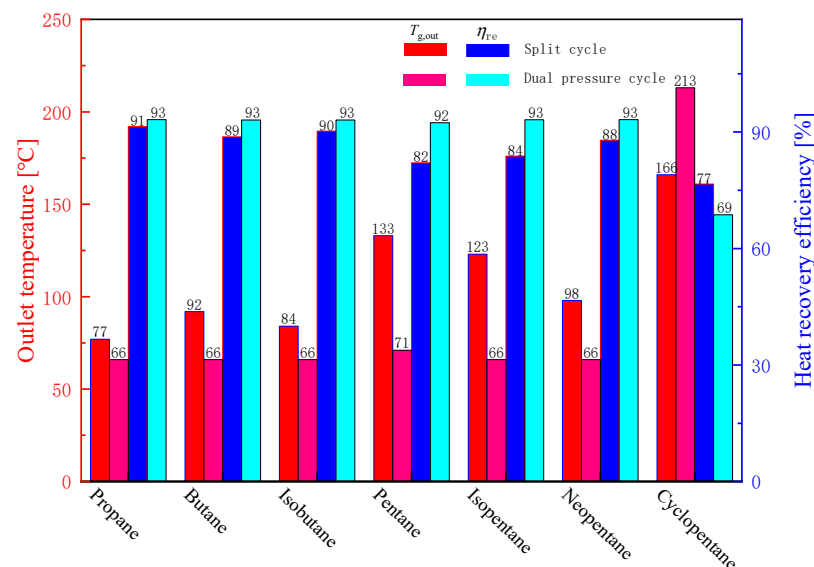


Figure 11. Waste heat recovery of split cycle and dual pressure cycle under design conditions.

Besides the waste heat recovery performance, system performances of split cycle and dual pressure cycle are also investigated for the considered working fluids. Figure 12 gives the histograms of net work, cycle efficiency and exergy efficiency for each working fluid. As presented in Figure 12, system performances vary greatly with the cycle layouts and the used working fluids. For the net work in Figure 12a, split cycle has higher values than the dual pressure cycle for most of working fluids, and the highest work, 48.71 kW, is obtained by the split cycle with butane, while the dual pressure cycle with propane has the lowest net work, 33.97 kW. For the cycle efficiency in Figure 12b and the exergy efficiency in Figure 12c, the split cycle has higher values than the dual pressure cycle at most of working fluids. However, the highest cycle efficiency, 29.62%, is obtained by the dual pressure cycle with cyclopentane, which is a little higher than 29.34% of the split cycle. Meanwhile, the dual pressure cycle with propane has the lowest cycle efficiency 17.98%. Being different with cycle efficiency, exergy efficiency 55.27% of cyclopentane is the largest in the split cycle. The lowest efficiency 37.67% is obtained by the dual pressure cycle with propane.

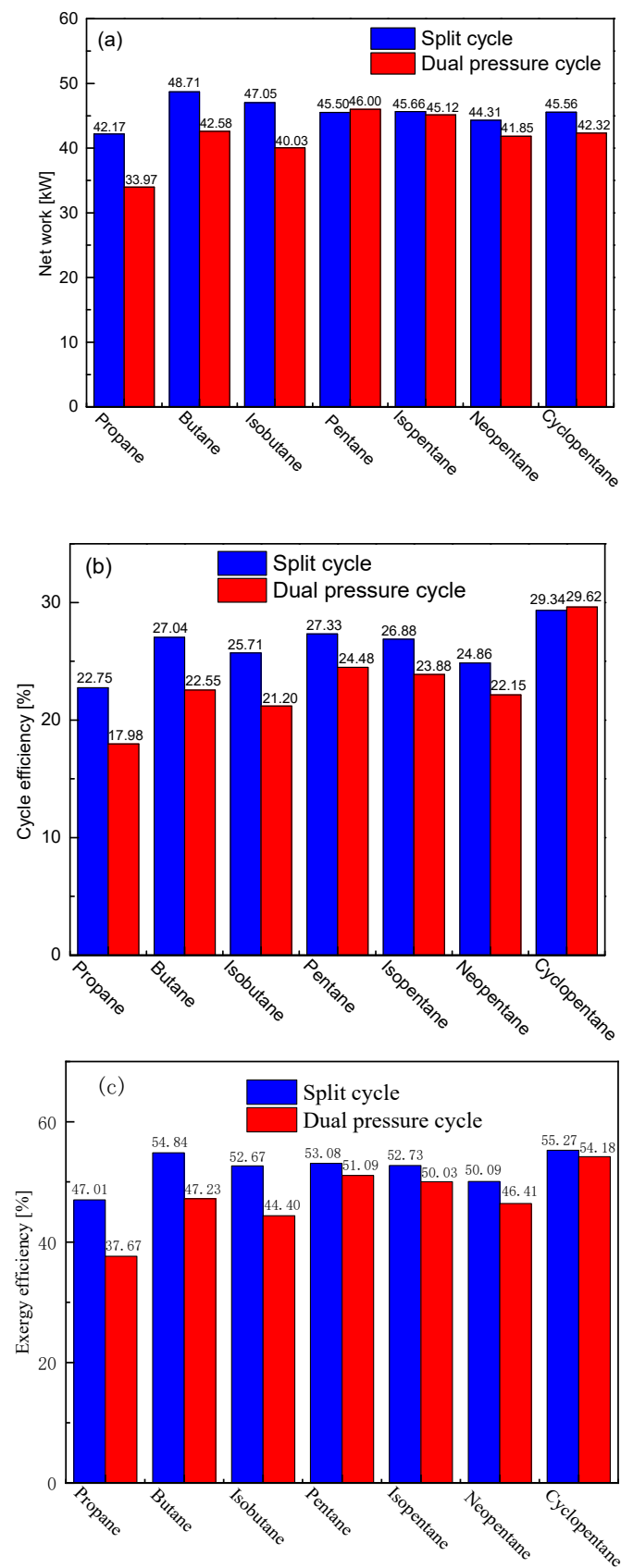


Figure 12. Cycle performances of split cycle and dual pressure cycle under design conditions (a) net work; (b) cycle efficiency; (c) exergy efficiency.

In order to discuss the heat exchange for heaters and recuperator, temperature distributions are derived for working fluids under design conditions. Considering the fact that the employed fluids almost have similar temperature curves, only pentane is used to illustrate the temperature distributions of these exchangers, as shown in Figure 13. For Heater1 in Figure 13a, the pinch point of Heater1 is always located at the cold end and the corresponding PPTD is 15 °C. Compared with the split cycle, the dual pressure cycle can extract more waste heat in Heater1. Additionally, the split cycle has a pinch point at the hot end of Heater2. This is because, compared with the Heater1, Heater2 has fewer mass flow rates of pentane, thus resulting in the fact that the total capacity of pentane is less than that of waste gas. On the other hand, due to the existence of evaporation in dual pressure cycle, the pinch point is located at the bubble point of working fluid. Before fluid evaporation, there is a good match between working fluid and waste gas. Figure 13b gives the temperature distributions of recuperator. Split cycle has a more uniform temperature distribution, and the temperature difference between working fluids is much lower than that of dual pressure cycle. This is caused by the fact that the mass flow rate of cold fluid in split cycle is greatly decreased, which reduces the heat capacity difference between the two sides of recuperator. Under design conditions, the pinch point of recuperator in split cycle is located at the hot end. However, for the dual pressure cycle, since the heat capacity of the hot flow is much smaller than that of the cold flow, the pinch point is at the cold end of the recuperator.

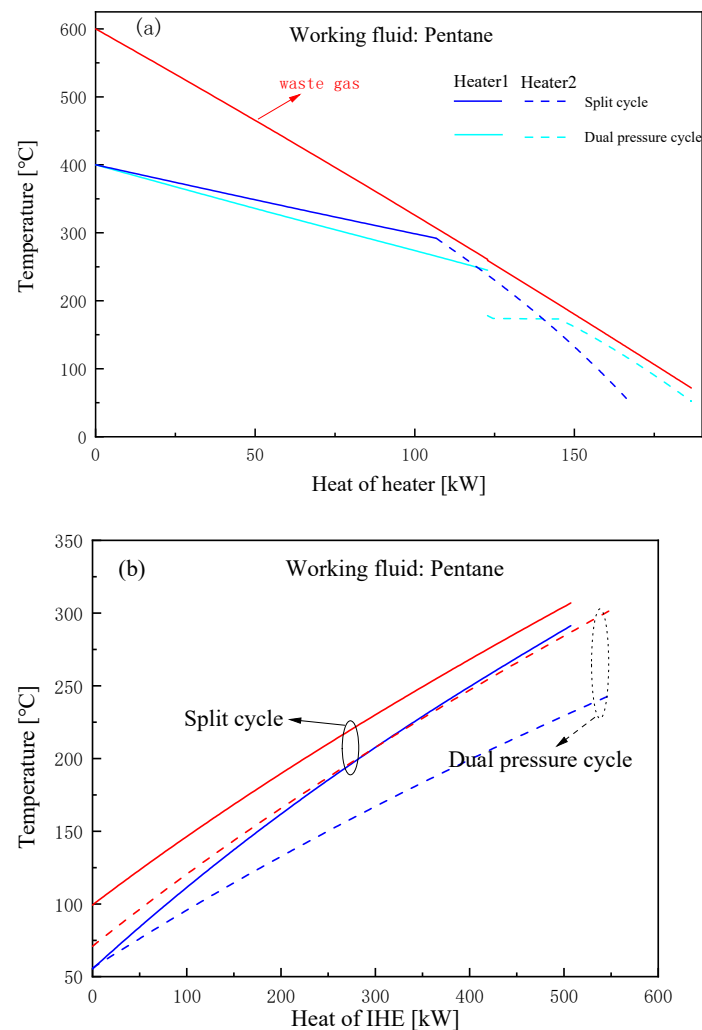


Figure 13. Temperature distributions of heat exchangers: (a) Heater; (b) IHE.

Based on the calculated energy parameters, exergy loss of each component in the two cycles is obtained for the considered working fluids. Take pentane as an example, Figure 14 shows the distribution of exergy loss for split cycle and dual pressure cycle. It can be concluded that for the split cycle, the highest exergy loss, 11.53 kW, occurs at Turbine1, followed by the condenser and Heater1. However, for the dual pressure cycle, the largest loss is obtained by the condenser, followed by Turbine1 and Heater1. As for the total exergy loss, the dual pressure cycle has a higher value than that of split cycle, due to the additional components: Turbine2 and Pump2.

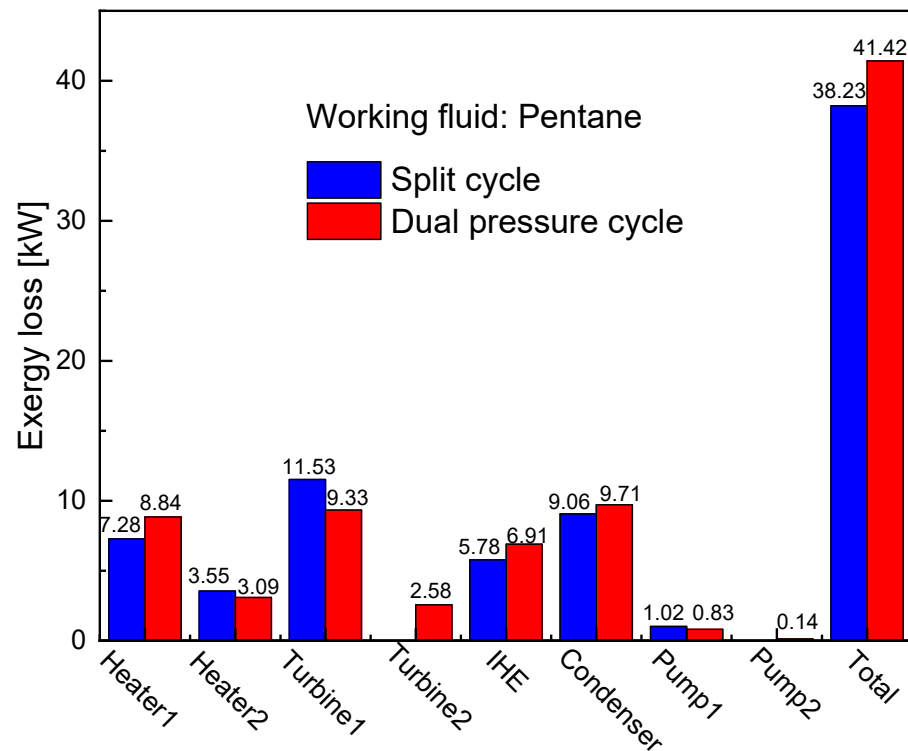


Figure 14. Exergy losses of different components for pentane under design conditions.

5.2. Effect of Turbine Inlet Temperature on Cycle Performances

For the considered two cycles, turbine inlet temperature (T_3), which is the highest operation temperature of system, has a significant impact on the system performance. Therefore, to reveal the impact of turbine inlet temperature, at different temperatures, system performances including net work, heat recovery efficiency, thermal efficiency and exergy efficiency are obtained by fixing other design parameters. Similarly, only pentane is considered here to illustrate the effect of turbine inlet temperature. The corresponding temperature varies from 300 °C to 550 °C at an interval of 25 °C.

The variation of net work with temperature is shown in Figure 15a. It can be observed that with the temperature increase, the net work of the two considered cycles first increases and then decreases. Although these two cycles have the same variation tendencies of net work, the variation range for the split cycle is greater than that for the dual pressure cycle. When the turbine inlet temperature is less than 375 °C, the split cycle has more produced work than the dual pressure cycle. Thereafter, the net work of the split cycle is gradually lower than that of the dual pressure cycle with the increase of temperature. Furthermore, at 425 °C, the net work reaches the highest, 45.66 kW for split cycle and 46.53 kW for dual pressure cycle. As for the heat recovery efficiency, opposite trends are observed for these two cycles. With the temperature increasing, the efficiency of the split cycle decreases, while the efficiency of the dual pressure cycle increases firstly and then keeps stable. Overall, when the temperature is larger than 375 °C, the dual pressure cycle has a larger efficiency than the split cycle. In addition, special care should be given to

the dual pressure cycle. There are no data points at 300 °C, due to the violation of pinch point constraint.

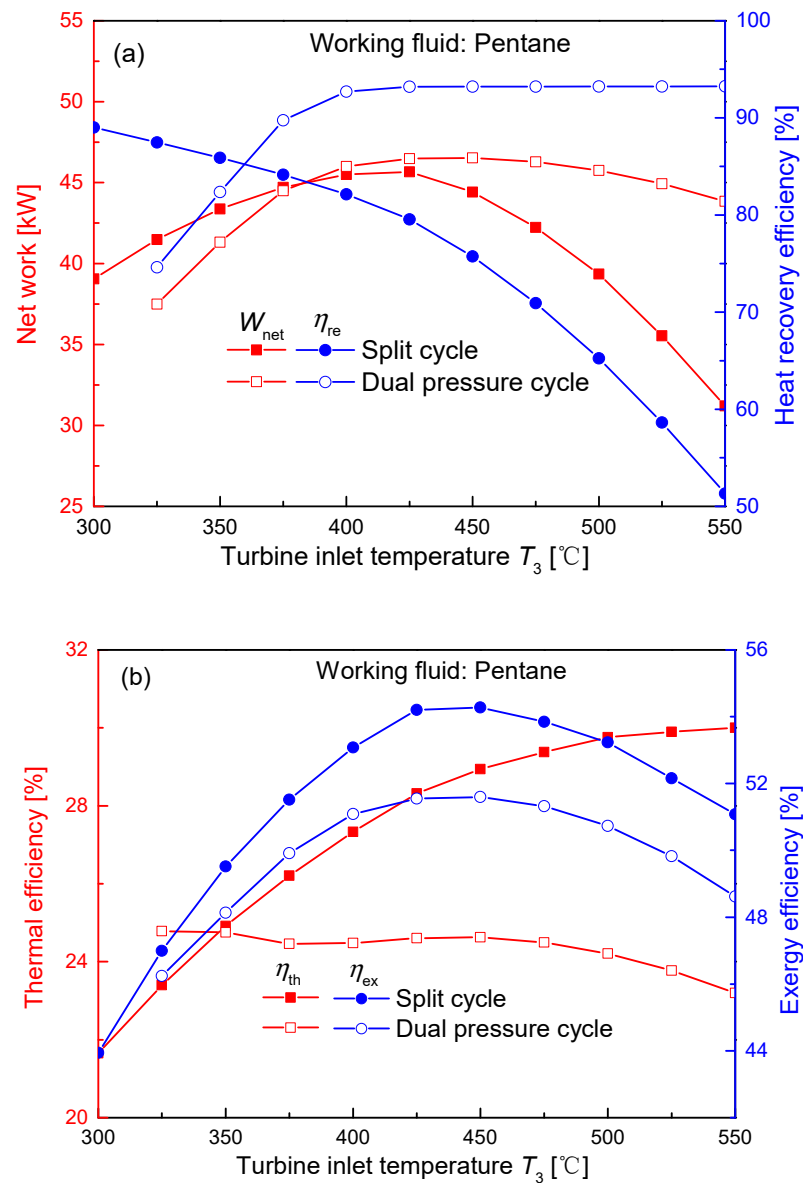


Figure 15. Effect of turbine inlet temperature on cycle performances: (a) net work and heat recovery efficiency; (b) thermal efficiency and exergy efficiency.

Figure 15b presents the variation curves of energy and exergy efficiencies for the split and dual pressure cycles. As the turbine inlet temperature increases, thermal efficiency of split cycle continuously goes up, while the dual pressure cycle has a slow downward trend of thermal efficiency overall. At a temperature higher than 350 °C, split cycle always has a higher thermal efficiency than dual pressure cycle. As for the exergy efficiency, the two cycles have similar variation trends. The efficiency increases firstly, then reaches the maximum value and lastly decreases. At 450 °C, maximum efficiencies are, respectively, 54.28%, 51.59% for split and dual pressure cycles. Furthermore, in the considered range of turbine inlet temperature, the exergy efficiency of split cycle is always larger than that of dual pressure cycle.

5.3. Effect of Turbine Inlet Pressure on Cycle Performances

In the transcritical ORC, the inlet pressure of turbine is independent of the corresponding temperature, while the outlet pressure of turbine is controlled by the condensation temperature. Therefore, the effect of turbine inlet pressure for both systems is investigated here. Under design conditions, with pentane as the working fluid, the turbine inlet pressure varies from 5 MPa to 15 MPa. The effect of pressure on cycle performances is shown in Figure 16. For the net work in Figure 16a, different variations are observed for the considered cycles. With the pressure increasing, net work of split cycle goes up to 50.32 kW firstly and then decreases, while the work of dual pressure cycle increases slowly and stabilizes around 46 kW. It can be found that when the pressure is less than 9 MPa, split cycle has a higher work than dual pressure cycle. As for the recovery efficiency, dual pressure cycle has higher values than split cycle in the considered ranges. Meanwhile, the efficiency variation of dual pressure cycle is less than that of split cycle. As the pressure increases from 5 MPa to 15 MPa, recovery efficiency of split cycle drops from 88.48% to 79.67%, while the efficiency of dual pressure cycle keeps around 92%.

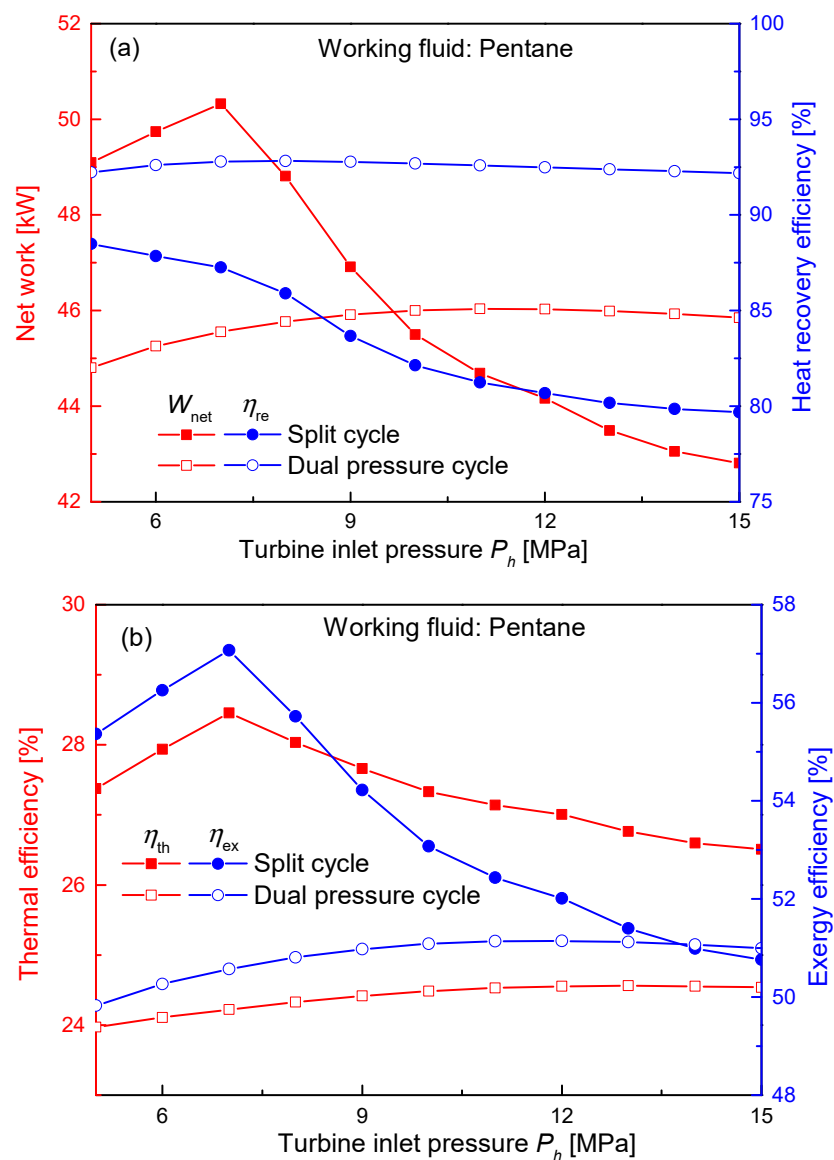


Figure 16. Effect of turbine inlet pressure on cycle performances: (a) net work and heat recovery efficiency; (b) thermal efficiency and exergy efficiency.

Figure 16b illustrates the variations of thermal efficiency and exergy efficiency with turbine inlet pressure. It can be observed that for the split cycle, both efficiencies increase firstly and then decrease. At 7 MPa, the maximum energy and exergy efficiencies are 28.45%, 57.07%, respectively. However, for the dual pressure cycle, both efficiencies slowly increase with the pressure, and stabilize around 24% and 51%, respectively. In terms of efficiency comparison between cycles, the split cycle always has a higher thermal efficiency than the dual pressure cycle. When the pressure is less than 14 MPa, the exergy efficiency of the split cycle is also larger than that of the dual pressure cycle.

5.4. Effect of Split Ratio on Performances of Split Cycle

In the above analysis, the split ratio is assumed to be 0.7 for the split cycle. However, in practical engineering, the split ratio can be easily controlled manually. When the ratio is 0, it means that the split cycle becomes the basic transcritical ORC. For the recuperative ORC, the split ratio corresponds to 1.0. Therefore, the effect of split ratio on split cycle performance is worth investigating.

Under design conditions, the split ratio varies between 0 and 1.0. Figure 17 shows the variations of split cycle performances. From Figure 17a, as the split ratio increases, the net work first increases and then decreases. The maximum net work, 45.50 kW, is achieved when the split ratio is 0.7. This result may be explained by the fact that at a smaller split ratio, the split cycle is more similar to the basic ORC, and the advantages of recuperator cannot be fully utilized. However, when the split ratio is close to 1.0, the split cycle is more similar to a recuperative cycle, and the advantage of splitting is weakened. As for the heat recovery efficiency, with the split ratio increasing, the efficiency at first barely changes and then decreases considerably. More working fluid enters Heater 2 when the split ratio is relatively small, so the recovery efficiency is high. After the split ratio increases to a certain extent, the cycle is close to the recuperative cycle, and more heat from working fluid is recuperated. Therefore, the recovery efficiency is reduced.

For the energy and exergy efficiencies, similar curves are obtained in Figure 17b. When the ratio is less than 0.8, the larger the split ratio, the higher the efficiencies. It can be explained by the fact that there is little change for the total absorbed heat in Heater1 and Heater2, while the net work goes up with the split ratio. Furthermore, at a split ratio greater than 0.8, both net work and absorbed heat are reduced, so that there are relatively small changes for these two efficiencies.

5.5. Effect of Evaporation Temperature on Performances of Dual Pressure Cycle

Being different with the split cycle, the dual pressure cycle has the evaporation temperature as a key parameter. In the above analysis, the evaporation temperature is fixed at $0.95 T_c$. However, the evaporation temperature directly determines the inlet temperature and pressure of Turbine2 in the dual pressure cycle, and has a significant influence on the cycle performance. Thus, here, the evaporation temperature is changed from $0.75 T_c$ to $0.95 T_c$ to reveal the effect, as illustrated in Figure 18.

Figure 18a shows that as the temperature ratio increases, the net work goes up from 40.54 kW to 46.00 kW, while the heat recovery efficiency drops from 93.42% to 92.69%. For the dual pressure cycle, the increase of net work is attributed to the subcritical cycle. At a higher evaporation temperature, more work can be produced by Turbine2. Furthermore, for the heat recovery efficiency, under the constraint of pinch point in Heater2, the increase of evaporation temperature will result into the outlet temperature increase of waste gas, thus decreasing the recovery efficiency. Similarly, due to the increase of net work and the reduction of recovered heat, Figure 18b indicates that the energy and exergy efficiencies increase with the temperature ratio.

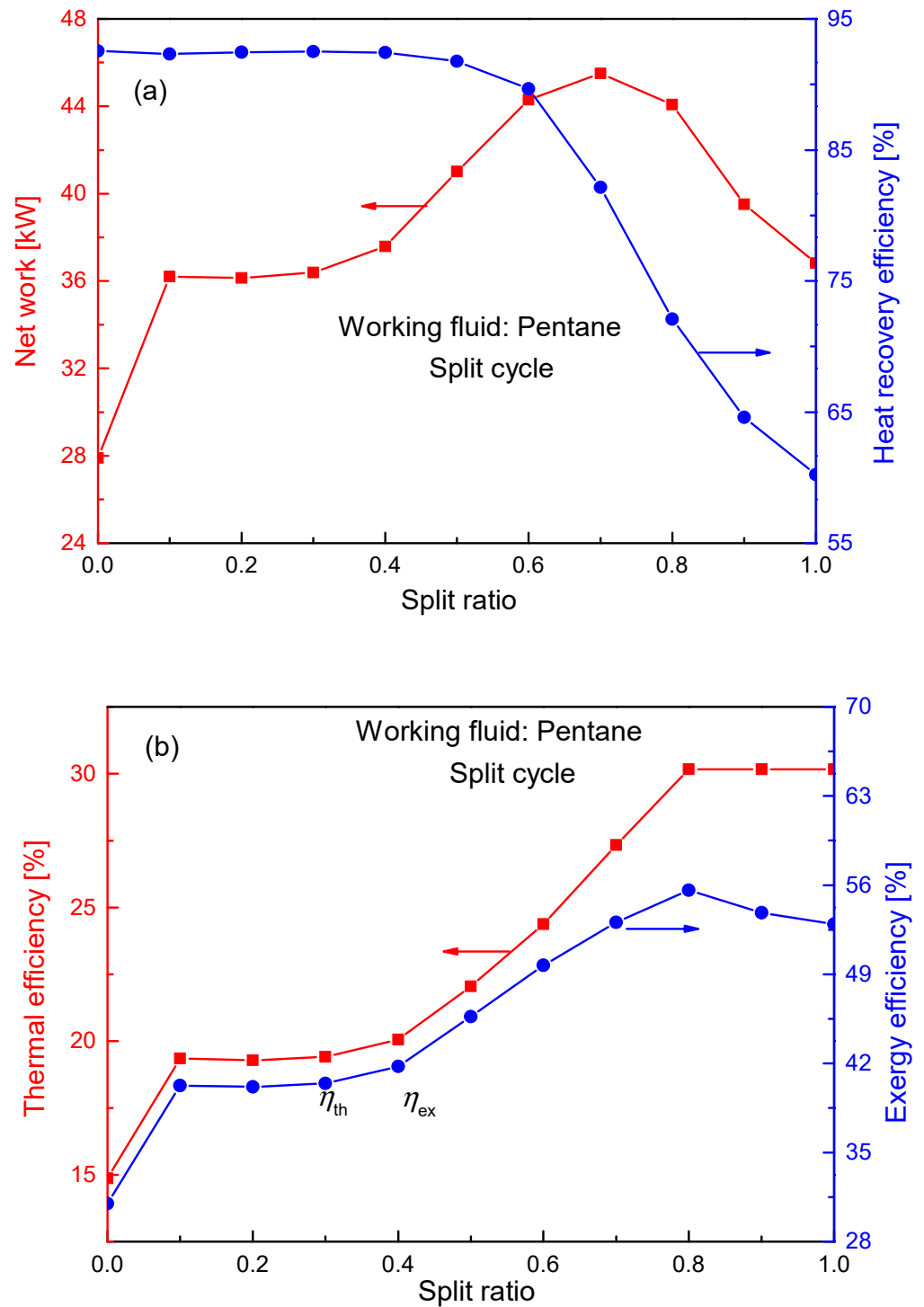


Figure 17. Effect of split ratio on performances of split cycle: (a) net work and heat recovery efficiency; (b) thermal efficiency and exergy efficiency.

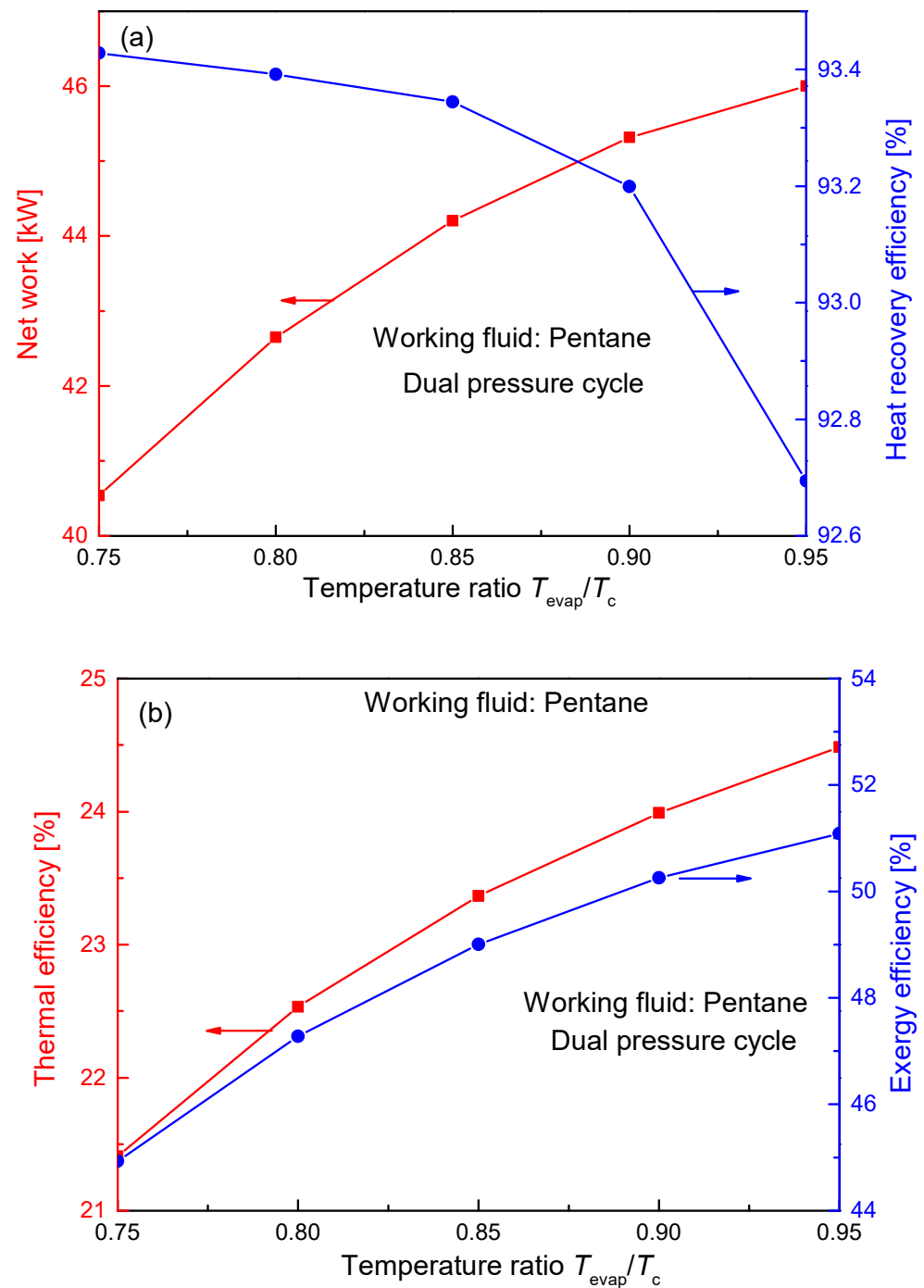


Figure 18. Effect of evaporation temperature on performances of dual pressure cycle: (a) net work and heat recovery efficiency; (b) thermal efficiency and exergy efficiency.

5.6. Effect of Condensation Temperatures on Cycle Performances

For the power cycle in the waste heat recovery of the mobile engine, the condensation temperature varies with the cooling methods. Thus, in this section, the performances of the split cycle and dual pressure cycle are analyzed at different condensation temperatures, namely 30 °C, 50 °C, 70 °C, and 90 °C, as presented in Figure 19.

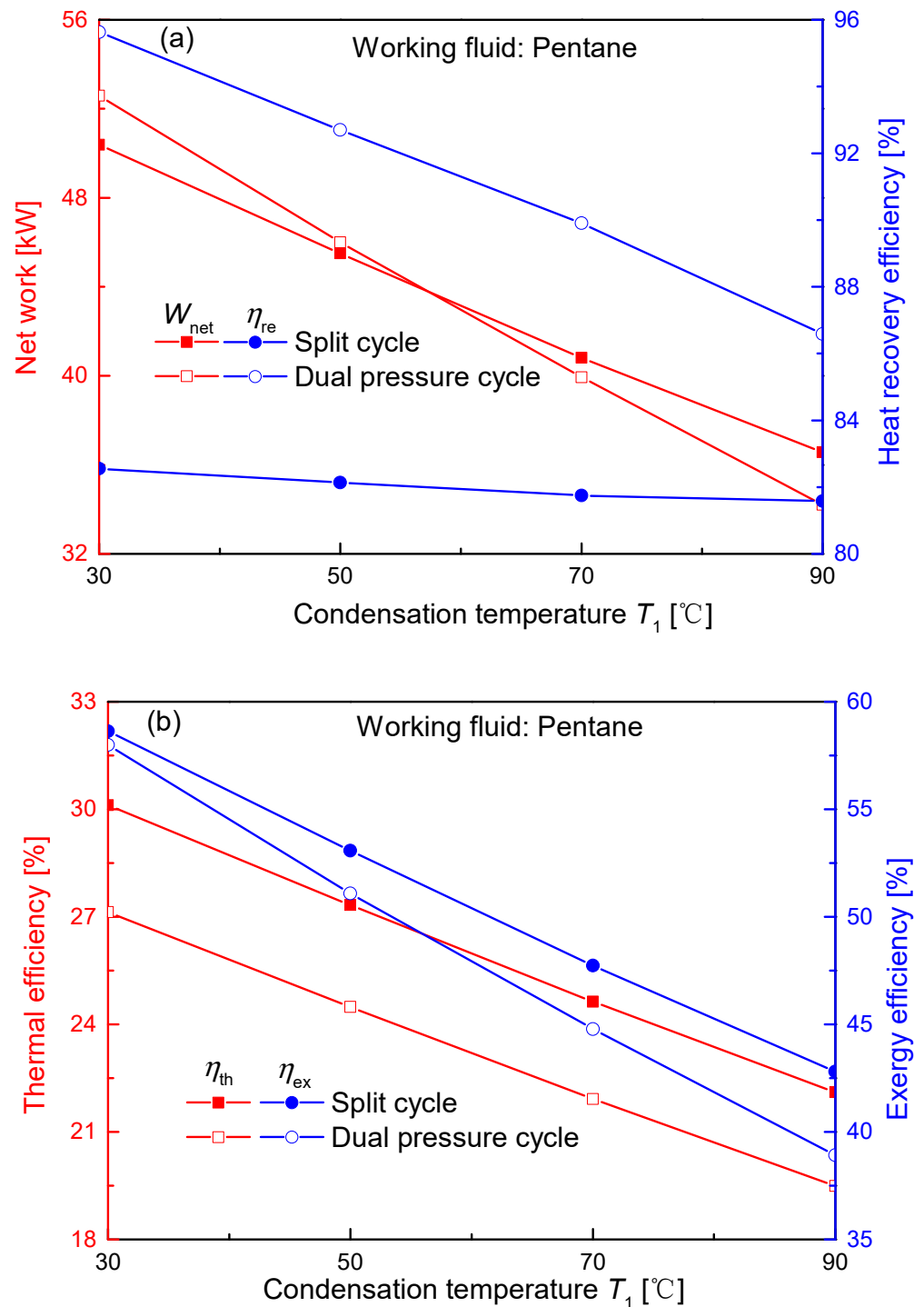


Figure 19. Effect of condensation temperature on cycle performances: (a) net work and heat recovery efficiency; (b) thermal efficiency and exergy efficiency.

Figure 19a shows that for every 20 °C increase in condensation temperature, the net work of the split cycle decreases by about 4.6 kW, while the net work of the dual pressure cycle decreases by about 6.12 kW. At a low condensation temperature, the dual pressure cycle has a larger work than the split cycle. However, at a higher condensation temperature, more work is produced by the split cycle. As for the recovery efficiency, the dual pressure cycle always has a larger value than the split cycle. For every 20 °C increase in condensation temperature, the recovery efficiency of the split cycle drops by about 0.32%, while the recovery efficiency of the dual pressure cycle drops by about 3.01%.

Figure 19b shows the variations of thermal efficiency and exergy efficiency. All these curves have decrease trends with the increase of condensation temperature. Meanwhile, efficiencies of the split cycle are higher than those of the dual pressure cycle. For the split cycle, as the condensation temperature is increased by 20 °C, the energy and exergy efficiencies are reduced by about 2.67% and 5.27%, respectively. For the dual pressure cycle, the efficiency reductions are around 2.55% and 6.36%, respectively. Theoretically, to improve the system performance, the condensation temperature should be as low as possible. However, the low temperature may result into a high system cost. Thus, in practical engineering, optimal condensation temperature should be determined by simultaneously considering the cycle performance and cost.

5.7. Effect of Turbomachinery Efficiency on Cycle Performances

In the performance calculation of thermodynamic cycles, efficiencies of the turbine and pump are always fixed at certain values. However, in practical engineering, due to the variation of operating conditions, the turbomachinery efficiency always deviates from the design value. In general, the less efficiency, the worse cycle performance. Therefore, effects of pump and turbine efficiencies on the cycle performances are investigated here. The corresponding efficiency varies from 0.5 to 0.9. Under design conditions, with pentane as the working fluid, performances of the two cycles in the considered range of efficiency are obtained, as listed in Tables 7 and 8.

Table 7. Effects of pump efficiency on cycle performances of pentane.

Pump Efficiency	Split Cycle			Dual Pressure Cycle		
	Net Work (kW)	Heat Recovery Efficiency (%)	Thermal Efficiency (%)	Net Work (kW)	Heat Recovery Efficiency (%)	Thermal Efficiency (%)
0.5	42.20	81.64	25.50	43.46	92.71	23.13
0.6	43.78	81.91	26.37	44.61	92.68	23.75
0.7	44.91	82.10	26.99	45.43	92.67	24.19
0.8	45.75	82.25	27.45	46.04	92.65	24.52
0.9	46.19	82.23	27.71	46.52	92.65	24.77

Table 8. Effects of turbine efficiency on cycle performances of pentane.

Turbine Efficiency	Split Cycle			Dual Pressure Cycle		
	Net Work (kW)	Heat Recovery Efficiency (%)	Thermal Efficiency (%)	Net Work (kW)	Heat Recovery Efficiency (%)	Thermal Efficiency (%)
0.5	35.37	86.30	20.22	36.61	93.22	19.38
0.6	40.71	83.90	23.94	41.52	93.18	21.99
0.7	45.76	82.25	27.45	46.04	92.65	24.52
0.8	50.19	80.91	30.61	50.34	92.12	26.96
0.9	54.33	79.95	33.53	54.48	91.71	29.31

Table 7 lists the net work, heat recovery efficiency and thermal efficiency of the two cycles at pump efficiency 0.5, 0.6, 0.7, 0.8 and 0.9. It can be easily observed that all performance indexes have small increases with the efficiency increase. In average, for split cycle, every 10% increase in pump efficiency, the net work increases 1 kW, while the two efficiencies increase 0.15% and 0.55%, respectively. For dual pressure cycle, 10% increase of pump efficiency can result into 0.79 kW increase of net work, 0.02% decrease of recovery efficiency, and 0.41% increase of thermal efficiency. Furthermore, it should be noted that in the range of pump efficiency, the net work of dual pressure cycle is always slightly higher than that of split cycle.

Table 8 gives the performance values at different turbine efficiencies. Compared with the pump efficiency, the turbine efficiency has much more influence on the system performances. For the split cycle, in the considered range of turbine efficiency, the net work

increases from 35.37 kW to 54.33 kW, while the thermal efficiency ranges 20.22~33.53%. Meanwhile, the heat recovery efficiency decreases from 86.30% to 79.95%. Similarly, for the dual pressure cycle, the net work and thermal efficiency, respectively, vary in the range of 36.61~54.48 kW and 19.38~29.31%, while the heat recovery efficiency decreases from 93.22% to 91.71%.

5.8. Parametric Optimization

The purpose of waste heat recovery is to generate as much power as possible. Thus, key parameters including turbine inlet temperature T_3 , turbine inlet pressure P_3 , split ratio SR and evaporation temperature T_{evap} are optimized using GA under the design conditions. For the condensation temperature, the optimal value is closely related with the system cost and the used cooling method. Thus, the condensation temperature is not discussed here. In the GA optimization, it is set to 50 °C. The turbine inlet temperature and pressure varies from 300 °C to 550 °C, 5 MPa to 15 MPa, respectively. For the split cycle, the range of split ratio is 0~1. While for the dual pressure cycle, the evaporation temperature varies from 0.75 T_c to 0.95 T_c . According to the optimization flowchart in Figure 8, with the target of maximum net work, these parameters are, respectively, optimized for split and dual pressure cycles.

Optimized results of the split cycle are summarized in Table 9 for the seven working fluids. It can be found that the maximum net works of these fluids are in the range 46.51~49.96 kW. The highest work is obtained by pentane, while the lowest work is achieved by propane. Furthermore, for the system parameters, optimal T_3 ranges from 381.73 °C to 427.90 °C. Except cyclopentane, optimal pressure for different working fluids decreases with the decrease of critical pressure. As for split ratio, it varies in the range of 0.66~0.76. With the goal to get the maximum work, the outlet temperature of waste gas generally increases from 77.65 °C to 146.07 °C, as the critical temperature increases. The corresponding recovery efficiency varies from 91.35% to 79.99%. For other system parameters, thermal efficiency is in the range of 25.12~30.69%, and exergy efficiency ranges 51.87~58.87%. After comparison among these working fluids, it's thought that pentane has the best performance of split cycle, in terms of net work.

Table 9. Optimized parameters of the split cycle.

Parameters	Propane	Butane	Isobutane	Pentane	Isopentane	Neopentane	Cyclopentane
T_3 (°C)	398.00	384.83	387.49	420.81	418.81	381.73	427.90
P_h (MPa)	10.11	9.04	7.95	6.17	7.12	7.50	7.35
SR	0.74	0.71	0.74	0.66	0.71	0.76	0.68
$T_{g,out}$ (°C)	77.65	87.90	82.33	90.08	112.59	101.77	146.07
m_f (kg/s)	0.39	0.34	0.40	0.30	0.31	0.39	0.25
W_{net} (kW)	46.51	49.86	49.72	49.96	49.22	48.36	49.75
η_{th} (%)	25.12	27.44	27.09	27.60	28.38	27.31	30.69
η_r (%)	91.35	89.65	90.57	89.29	85.56	87.36	79.99
η_{ex} (%)	51.87	55.96	55.61	56.15	56.29	54.82	58.87

For the dual pressure cycle, optimized parameters are summarized in Table 10. Compared with the split cycle, dual pressure cycle has a larger difference of net work for different working fluids. The corresponding range is 36.04~52.05 kW. Maximum and minimum values are, respectively, obtained by propane and cyclopentane. Furthermore, for all working fluids, optimal pressure and evaporation temperature are 15 MPa, 0.95 T_c , respectively. The outlet temperatures of waste gas are all around 66 °C, and the corresponding recovery efficiency is around 93%. A large difference exists for optimal T_3 . As the critical temperature of working fluid increases, the optimal temperature increases from 400.30 °C to 516.26 °C. As for other parameters, variation ranges of energy and exergy efficiencies are 19.08~27.56% and 39.97~57.73%, respectively. For the performance comparison between the two cycles, the split cycle always has a higher work than the dual pressure

cycle for the considered fluids except cyclopentane. Thus, the split cycle is recommended in the application of waste heat recovery, due to the higher net work and fewer system components.

Table 10. Optimized parameters of the dual pressure cycle.

Parameters	Propane	Butane	Isobutane	Pentane	Isopentane	Neopentane	Cyclopentane
T_3 (°C)	400.30	430.88	425.89	450.87	440.31	416.95	516.26
P_h (MPa)	15.00	15.00	15.00	15.00	15.00	15.00	15.00
T_{evap}/T_c	0.95	0.95	0.95	0.95	0.95	0.95	0.95
$T_{g,out}$ (°C)	66.33	66.59	66.42	66.31	66.34	66.31	66.55
m_{f1} (kg/s)	0.25	0.20	0.22	0.19	0.20	0.23	0.15
m_{f2} (kg/s)	0.22	0.17	0.21	0.15	0.16	0.19	0.16
W_{net} (kW)	36.04	43.33	40.72	46.81	45.63	42.15	52.05
η_{th} (%)	19.08	22.94	21.56	24.78	24.15	22.31	27.56
η_r (%)	93.21	93.17	93.20	93.22	93.21	93.22	93.18
η_{ex} (%)	39.97	48.05	45.16	51.91	50.60	46.74	57.73

6. Conclusions

In this paper, two advanced transcritical cycles, namely split cycle and dual pressure cycle, are employed to deeply extract the waste heat from a mobile engine, on the basis of recuperative cycle. To recover the heat efficiently and avoid the fluid decomposition, seven high-temperature working fluids are selected. Under given gas conditions of the engine, performances of seven working fluids in these two cycles are analyzed. On this basis, effects of turbine inlet temperature and pressure, split ratio, evaporation temperature, condensation temperature and turbomachinery efficiency on performances of the two cycles are investigated. In addition, key parameters are optimized using net work as a fitness function of GA. According to the above analysis, the following conclusions can be drawn.

- (1) Under design conditions, the dual pressure cycle can extract more waste heat than the split cycle for most high-temperature fluids. However, a higher net work is generally achieved by the split cycle. Among the considered fluids, the highest work 48.71 kW, is obtained by the split cycle with butane.
- (2) As the turbine inlet temperature increases, the net work of considered two cycles first increases and then decreases. Meanwhile, with the turbine inlet pressure increasing, net work of split cycle first goes up and then decreases, while the work of dual pressure cycle increases slowly.
- (3) For the split cycle, an optimal split ratio exists to get the maximum network. For the dual pressure cycle, as the evaporation temperature increases, performances except recovery efficiency increases. Furthermore, with the condensation temperature increasing and the turbomachinery efficiency decreasing, thermodynamic performances including net work and efficiency have different reduction degrees.
- (4) For the selected seven working fluids, optimized net works are in the range 46.51~49.96 kW for the split cycle. The highest work is obtained by pentane, while the lowest work is achieved by propane. As for the dual pressure cycle, the work range is 36.04~52.05 kW. The minimum and maximum values are, respectively, obtained by propane and cyclopentane. At the same fluid except cyclopentane, split cycle always has a higher work than dual pressure cycle. Meanwhile, with the advantage of fewer components, split cycle is recommended to recover the waste heat of ICE.

Aiming at the off design conditions of ICE, I further work will focus on system performance degradation and dynamic simulation. On this basis, control strategies will be investigated to assure the high-efficient and safe operation. Furthermore, for the cycle layouts, intelligent construction of cycle structures should be conducted, based on the advanced algorithm and machine learning. Thereafter, system cost should be considered in

detail. As for the selection of high-temperature working fluids, computer-aided molecular design should be paid more attention to realize the fluid design for the waste heat recovery of transcritical ORC.

Author Contributions: Writing—original draft preparation, X.L.; methodology, C.C.; formal analysis, A.Y.; Conceptualization, L.Y.; writing—review and editing, W.S. All authors have read and agreed to the published version of the manuscript.

Funding: This research was funded by the program “National Nature Science Foundation of China”, grant number 52106037 and “Researches on key technology to optimization and dynamic simulation of supercritical CO₂ power cycle”, grant number 202003024.

Institutional Review Board Statement: Not applicable.

Informed Consent Statement: Not applicable.

Data Availability Statement: Not applicable.

Conflicts of Interest: The authors declare no conflict of interest.

Nomenclature

Symbols

h	Specific enthalpy (kJ/kg)
m	Mass flow rate (kg/s)
E	Exergy (kW)
I	Irreversibility or exergy destruction rate (kW)
M	Molecular weight (g/mol)
P	Pressure (MPa)
Q	Heat transfer rate (kW)
s	Entropy (kJ/(kg·K))
T	Temperature (K or °C)
W	Work down, power (kW)

Greeks

η	Efficiency (%)
Δ	Difference

Abbreviations

GA	Genetic algorithm
ICE	Internal combustion engine
IHE	Internal heat exchanger
ORC	Organic Rankine cycle
HT	How-temperature
LT	Low-temperature
SR	Split ratio
PPTD	Pinch point temperature difference
S-CO ₂	Supercritical carbon dioxide

Subscripts and superscripts

c	Critical state
C	Condenser
Con	Condensation
Com	compressor
f	Working fluid
g	Exhaust gas
$H1$	Heater 1
$H2$	Hever 2
$T1$	Turbine 1
$T2$	Turbine 2
$P1$	Pump 1
$P2$	Pump 2

<i>h</i>	High pressure
<i>i</i>	A state point of a cycle
<i>in</i>	Inlet temperature of gas
<i>mid</i>	Temperature at the outlet of Heater1
<i>net</i>	Net value
<i>evap</i>	Evaporation
<i>out</i>	Outlet temperature of gas
<i>ex</i>	Exergy
<i>re</i>	Recovery
<i>th</i>	Thermodynamic
1, ... 8	Thermodynamic state points

Appendix A

Based on the published literature, 32 commonly used working fluids are summarized in Table A1.

Table A1. 32 high-temperature working fluids.

Working Fluid	Structure	<i>M</i> (g/mol)	<i>T_c</i> (°C)	<i>P_c</i> (kPa)	<i>P_{con}</i> at 50 °C (kPa)
Ethane	CH ₃ CH ₃	30.07	32.17	4872.20	—
Propane	CH ₃ CH ₂ CH ₃	44.10	96.74	4251.20	1713.30
Butane	CH ₃ -2(CH ₂)-CH ₃	58.12	151.98	3796.00	495.75
Isobutane	CH(CH ₃) ₃	58.12	134.66	3629.00	684.90
Pentane	CH ₃ -3(CH ₂)-CH ₃	72.15	196.55	3370.00	159.25
Isopentane	(CH ₃) ₂ CHCH ₂ CH ₃	72.15	187.20	3378.00	205.51
Neopentane	C(CH ₃) ₄	72.15	160.59	3196.00	355.80
Cyclopentane	C ₅ H ₁₀	70.13	238.57	4571.20	103.83
Isohexane	(CH ₃) ₂ CH(CH ₂) ₂ CH ₃	86.18	224.55	3040.00	72.33
Hexane	CH ₃ -4(CH ₂)-CH ₃	86.18	234.67	3034.00	54.09
Cyclohexane	C ₆ H ₁₂	84.16	280.45	4080.50	36.27
Heptane	CH ₃ -5(CH ₂)-CH ₃	100.20	266.98	2736.00	18.88
Octane	CH ₃ -6(CH ₂)-CH ₃	114.23	296.17	2497.00	6.68
Nonane	CH ₃ -7(CH ₂)-CH ₃	128.26	321.40	2281.00	2.42
Decane	CH ₃ -8(CH ₂)-CH ₃	142.28	344.55	2103.00	0.88
Dodecane	CH ₃ -10(CH ₂)-CH ₃	170.33	384.95	1817.00	0.12
Benzene	C ₆ H ₆	78.11	288.87	4907.30	36.20
Toluene	CH ₃ -C ₆ H ₅	92.14	318.60	4126.30	12.29
Methylcyclohexane	C ₆ H ₁₁ -CH ₃	98.19	299.05	3470.00	18.44
Ethyl benzene	C ₈ H ₁₀	106.17	343.97	3622.40	4.69
m-xylene	C ₈ H ₁₀ -1.3-dimethylbenzene	106.17	343.74	3534.60	4.16
p-xylene	C ₈ H ₁₀ -1.4-dimethylbenzene	106.17	343.02	3531.50	4.35
MM	C ₆ H ₁₈ OSI ₂	162.38	245.60	1939.00	17.49
MDM	C ₈ H ₂₄ O ₂ SI ₃	236.53	290.94	1415.00	2.19
MD2M	C ₁₀ H ₃₀ O ₃ SI ₄	310.69	326.25	1227.00	0.33
MD3M	C ₁₂ H ₃₆ O ₄ SI ₅	384.84	355.21	945.00	0.05
MD4M	C ₁₄ H ₄₂ O ₅ SI ₆	458.99	380.05	877.00	0.00
D4	C ₈ H ₂₄ O ₄ SI ₄	296.62	313.35	1332.00	0.70
D5	C ₁₀ H ₃₀ O ₅ SI ₅	370.77	346.00	1160.00	0.15
D6	C ₁₂ H ₃₆ O ₆ SI ₆	444.92	372.63	961.00	0.03
Methanol	CH ₃ OH	32.04	239.45	8103.50	55.68
Ethanol	C ₂ H ₆ O	46.07	241.56	6268.00	29.41
Acetone	(CH ₃) ₂ CO	58.08	234.95	4700.00	81.95

References

1. Zhang, R.; Su, W.; Lin, X.; Zhou, N.; Zhao, L. Thermodynamic analysis and parametric optimization of a novel S–CO₂ power cycle for the waste heat recovery of internal combustion engines. *Energy* **2020**, *209*, 118484. [[CrossRef](#)]
2. Zhu, S.; Zhang, K.; Deng, K. A review of waste heat recovery from the marine engine with highly efficient bottoming power cycles. *Renew. Sustain. Energy Rev.* **2020**, *120*, 109611. [[CrossRef](#)]
3. Lan, Q.; Bai, Y.; Fan, L.; Gu, Y.; Wen, L.; Yang, L. Investigation on fuel injection quantity of low-speed diesel engine fuel system based on response surface prediction model. *Energy* **2020**, *211*, 118946. [[CrossRef](#)]
4. Shi, L.; Shu, G.; Tian, H.; Deng, S. A review of modified Organic Rankine cycles (ORCs) for internal combustion engine waste heat recovery (ICE-WHR). *Renew. Sustain. Energy Rev.* **2018**, *92*, 95–110. [[CrossRef](#)]
5. Fraioli, V.; Beatrice, C.; Di Blasio, G.; Belgiorno, G.; Migliaccio, M. *Multidimensional Simulations of Combustion in Methane-Diesel Dual-Fuel Light-Duty Engines*; SAE International: Warrendale, PA, USA, 2017.
6. Xu, B.; Li, X. A Q-learning based transient power optimization method for organic Rankine cycle waste heat recovery system in heavy duty diesel engine applications. *Appl. Energy* **2021**, *286*, 116532. [[CrossRef](#)]
7. Hernandez, A.; Ruiz, F.; Gusev, S.; De Keyser, R.; Quoilin, S.; Lemort, V. Experimental validation of a multiple model predictive control for waste heat recovery organic Rankine cycle systems. *Appl. Therm. Eng.* **2021**, *193*, 116993. [[CrossRef](#)]
8. Peralez, J.; Nadri, M.; Dufour, P.; Tona, P.; Sciarretta, A. Organic Rankine Cycle for Vehicles: Control Design and Experimental Results. *IEEE Trans. Control Syst. Technol.* **2017**, *25*, 952–965. [[CrossRef](#)]
9. Zhang, Y.-Q.; Wu, Y.; Xia, G.; Ma, C.-F.; Ji, W.-N.; Liu, S.-W.; Yang, K.; Yang, F.-B. Development and experimental study on organic Rankine cycle system with single-screw expander for waste heat recovery from exhaust of diesel engine. *Energy* **2014**, *77*, 499–508. [[CrossRef](#)]
10. Liu, P.; Shu, G.; Tian, H. Carbon Dioxide as Working Fluids in Transcritical Rankine Cycle for Diesel Engine Multiple Waste Heat Recovery in Comparison to Hydrocarbons. *J. Therm. Sci.* **2019**, *28*, 494–504. [[CrossRef](#)]
11. Yağlı, H.; Koç, Y.; Koç, A.; Görgülü, A.; Tandiroğlu, A. Parametric optimization and exergetic analysis comparison of subcritical and supercritical organic Rankine cycle (ORC) for biogas fuelled combined heat and power (CHP) engine exhaust gas waste heat. *Energy* **2016**, *111*, 923–932. [[CrossRef](#)]
12. Yang, M.H. Optimizations of the waste heat recovery system for a large marine diesel engine based on transcritical Rankine cycle. *Energy* **2016**, *113*, 1109–1124. [[CrossRef](#)]
13. Yang, M.H.; Yeh, R.H. Economic research of the transcritical Rankine cycle systems to recover waste heat from the marine medium-speed diesel engine. *Appl. Therm. Eng.* **2017**, *114*, 1343–1354. [[CrossRef](#)]
14. Tian, H.; Liu, P.; Shu, G. Challenges and opportunities of Rankine cycle for waste heat recovery from internal combustion engine. *Prog. Energy Combust. Sci.* **2021**, *84*, 100906. [[CrossRef](#)]
15. Shu, G.; Shi, L.; Tian, H.; Deng, S.; Li, X.; Chang, L. Configurations selection maps of CO₂-based transcritical Rankine cycle (CTRC) for thermal energy management of engine waste heat. *Appl. Energy* **2017**, *186*, 423–435. [[CrossRef](#)]
16. Li, L.; Tian, H.; Liu, P.; Shi, L.; Shu, G. Optimization of CO₂ Transcritical Power Cycle (CTPC) for engine waste heat recovery based on split concept. *Energy* **2021**, *229*, 120718. [[CrossRef](#)]
17. Tian, H.; Liu, L.; Shu, G.; Wei, H.; Liang, X. Theoretical research on working fluid selection for a high-temperature regenerative transcritical dual-loop engine organic Rankine cycle. *Energy Convers. Manag.* **2014**, *86*, 764–773. [[CrossRef](#)]
18. Song, J.; Li, X.; Wang, K.; Markides, C.N. Parametric optimisation of a combined supercritical CO₂ (S-CO₂) cycle and organic Rankine cycle (ORC) system for internal combustion engine (ICE) waste-heat recovery. *Energy Convers. Manag.* **2020**, *218*, 112999. [[CrossRef](#)]
19. Di Battista, D.; Fatigati, F.; Carapellucci, R.; Cipollone, R. An improvement to waste heat recovery in internal combustion engines via combined technologies. *Energy Convers. Manag.* **2021**, *232*, 113880. [[CrossRef](#)]
20. Chen, T.; Zhuge, W.; Zhang, Y.; Zhang, L. A novel cascade organic Rankine cycle (ORC) system for waste heat recovery of truck diesel engines. *Energy Convers. Manag.* **2017**, *138*, 210–223. [[CrossRef](#)]
21. Liu, P.; Shu, G.; Tian, H. How to approach optimal practical Organic Rankine cycle (OP-ORC) by configuration modification for diesel engine waste heat recovery. *Energy* **2019**, *174*, 543–552. [[CrossRef](#)]
22. Grelet, V.; Reiche, T.; Lemort, V.; Nadri, M.; Dufour, P. Transient performance evaluation of waste heat recovery rankine cycle based system for heavy duty trucks. *Appl. Energy* **2016**, *165*, 878–892. [[CrossRef](#)]
23. Dai, X.; Shi, L.; Qian, W. Review of the working fluid thermal stability for Organic Rankine Cycles. *J. Therm. Sci.* **2019**, *28*, 597–607. [[CrossRef](#)]
24. Benato, A.; Kærn, M.R.; Pierobon, L.; Stoppato, A.; Haglind, F. Analysis of hot spots in boilers of organic Rankine cycle units during transient operation. *Appl. Energy* **2015**, *151*, 119–131. [[CrossRef](#)]
25. Wang, X.; Tian, H.; Shu, G. Part-Load Performance Prediction and Operation Strategy Design of Organic Rankine Cycles with a Medium Cycle Used for Recovering Waste Heat from Gaseous Fuel Engines. *Energies* **2016**, *9*, 10. [[CrossRef](#)]
26. Shu, G.; Zhao, M.; Tian, H.; Wei, H.; Liang, X.; Huo, Y.; Zhu, W. Experimental investigation on thermal OS/ORC (Oil Storage/Organic Rankine Cycle) system for waste heat recovery from diesel engine. *Energy* **2016**, *107*, 693–706. [[CrossRef](#)]
27. Shu, G.; Li, X.; Tian, H.; Liang, X.; Wei, H.; Wang, X. Alkanes as working fluids for high-temperature exhaust heat recovery of diesel engine using organic Rankine cycle. *Appl. Energy* **2014**, *119*, 204–217. [[CrossRef](#)]

28. Shu, G.; Liu, L.; Tian, H.; Wei, H.; Liang, Y. Analysis of regenerative dual-loop organic Rankine cycles (DORCs) used in engine waste heat recovery. *Energy Convers. Manag.* **2013**, *76*, 234–243. [[CrossRef](#)]
29. Li, X.; Shu, G.; Tian, H.; Huang, G.; Liu, P.; Wang, X.; Shi, L. Experimental comparison of dynamic responses of CO₂ transcritical power cycle systems used for engine waste heat recovery. *Energy Convers. Manag.* **2018**, *161*, 254–265. [[CrossRef](#)]
30. Pan, L.; Shi, W.; Wei, X.; Li, T.; Li, B. Experimental verification of the self-condensing CO₂ transcritical power cycle. *Energy* **2020**, *198*, 117335. [[CrossRef](#)]
31. Wang, M.; Zhang, J.; Zhao, S.; Liu, Q.; Zhao, Y.; Wu, H. Performance investigation of transcritical and dual-pressure Organic Rankine Cycles from the aspect of thermal match. *Energy Convers. Manag.* **2019**, *197*, 111850. [[CrossRef](#)]
32. Zhang, Q.; Luo, Z.; Zhao, Y.; Pavel, S. Thermodynamic analysis and multi-objective optimization of a transcritical CO₂ waste heat recovery system for cruise ship application. *Energy Convers. Manag.* **2021**, *227*, 113612. [[CrossRef](#)]
33. Houck, C.R.; Joines, J.; Kay, M.G. A genetic algorithm for function optimization: A Matlab implementation. *NCSU.IE. TR* **2008**, *9*, 95.
34. Van Kleef, L.M.T.; Oyewunmi, O.A.; Markides, C.N. Multi-objective thermo-economic optimization of organic Rankine cycle (ORC) power systems in waste-heat recovery applications using computer-aided molecular design techniques. *Appl. Energy* **2019**, *251*, 112513. [[CrossRef](#)]
35. Jankowski, M.; Borsukiewicz, A.; Wiśniewski, S.; Hooman, K. Multi-objective analysis of an influence of a geothermal water salinity on optimal operating parameters in low-temperature ORC power plant. *Energy* **2020**, *202*, 117666. [[CrossRef](#)]
36. Razmi, A.R.; Arabkoohsar, A.; Nami, H. Thermoeconomic analysis and multi-objective optimization of a novel hybrid absorption/recompression refrigeration system. *Energy* **2020**, *210*, 118559. [[CrossRef](#)]
37. Liu, X.; Nguyen, M.Q.; He, M. Performance analysis and optimization of an electricity-cooling cogeneration system for waste heat recovery of marine engine. *Energy Convers. Manag.* **2020**, *214*, 112887. [[CrossRef](#)]
38. Balafkandeh, S.; Zare, V.; Gholamian, E. Multi-objective optimization of a tri-generation system based on biomass gasification/digestion combined with S-CO₂ cycle and absorption chiller. *Energy Convers. Manag.* **2019**, *200*, 112057. [[CrossRef](#)]
39. Lemmon, E.W.; Bell, I.H.; Huber, M.L.; McLinden, M.O. *NIST Standard Reference Database 23, Reference Fluid Thermodynamic and Transport Properties-REFPROP, Version 10.0*, National Institute of Standards and Technology; Standard Reference Data Program: Gaithersburg, MD, USA, 2018.